CONCLUSION

Based on the results of this study, we conclude that NP-L33s has a lower propensity than NP-L20 to induce the ABC phenomenon and a good sustained-release profile of PGE_1, which may be clinically useful.

ACKNOWLEDGEMENTS

This work was supported by Grants-in-Aid for Scientific Research from the Ministry of Health, Labour, and Welfare of Japan, as well as the Japan Science and Technology Agency and Grants-in-Aid for Scientific Research from the Ministry of Education, Culture, Sports, Science and Technology, Japan.

REFERENCES

1. Maeda H, Wu J, Sawa T, Matsumura Y, Hori K. Tumor vascular permeability and the EPR effect in macromolecular therapeutics: a review. J Control Release. 2000;65:271–84.
2. Gref R, Minamitake Y, Peracchia MT, Trubetskoy V, Torchilin V, Langer R. Biodegradable long-circulating polymeric nanospheres. Science 1994;263:1600–3.
3. Stolnik S, Dunn SE, Garnett MC, Davies MC, Coombes AG, Taylor DC, *et al.* Surface modification of poly(lactide-co-glycolide) nanospheres by biodegradable poly(lactide)-poly(ethylene glycol) copolymers. Pharm Res. 1994;11:1800–8.
4. Ishihara T, Takahashi M, Higaki M, Takenaga M, Mizushima T, Mizushima Y. Prolonging the *in vivo* residence time of prostaglandin E(1) with biodegradable nanoparticles. Pharm Res. 2008;25:1686–95.
5. Sharpe M, Easthope SE, Keating GM, Lamb HM. Polyethylene glycol-liposomal doxorubicin: a review of its use in the management of solid and haematological malignancies and AIDS-related Kaposi's sarcoma. Drugs 2002;62:2089–126.
6. Dams ET, Laverman P, Oyen WJ, Storm G, Scherphof GL, van Der Meer JW, *et al.* Accelerated blood clearance and altered biodistribution of repeated injections of sterically stabilized liposomes. J Pharmacol Exp Ther. 2000;292:1071–9.
7. Ishida T, Maeda R, Ichihara M, Mukai Y, Motoki Y, Manabe Y, *et al.* The accelerated clearance on repeated injection of pegylated liposomes in rats: laboratory and histopathological study. Cell Mol Biol Lett. 2002;7:286.
8. Ishida T, Kiwada H. Accelerated blood clearance (ABC) phenomenon upon repeated injection of PEGylated liposomes. Int J Pharm. 2008;354:56–62.
9. Wang XY, Ishida T, Ichihara M, Kiwada H. Influence of the physicochemical properties of liposomes on the accelerated blood clearance phenomenon in rats. J Control Release. 2005;104:91–102.
10. Laverman P, Carstens MG, Boerman OC, Dams ET, Oyen WJ, van Rooijen N, *et al.* Factors affecting the accelerated blood clearance of polyethylene glycol-liposomes upon repeated injection. J Pharmacol Exp Ther. 2001;298:607–12.
11. Ishida T, Ichihara M, Wang X, Yamamoto K, Kimura J, Majima E, *et al.* Injection of PEGylated liposomes in rats elicits PEG-specific IgM, which is responsible for rapid elimination of a second dose of PEGylated liposomes. J Control Release. 2006;112:15–25.
12. Ishida T, Atobe K, Wang X, Kiwada H. Accelerated blood clearance of PEGylated liposomes upon repeated injections: effect of doxorubicin-encapsulation and high-dose first injection. J Control Release. 2006;115:251–8.
13. Ishida T, Masuda K, Ichikawa T, Ichihara M, Irimura K, Kiwada H. Accelerated clearance of a second injection of PEGylated liposomes in mice. Int J Pharm. 2003;255:167–74.
14. Ishida T, Maeda R, Ichihara M, Irimura K, Kiwada H. Accelerated clearance of PEGylated liposomes in rats after repeated injections. J Control Release. 2003;88:35–42.
15. Wang X, Ishida T, Kiwada H. Anti-PEG IgM elicited by injection of liposomes is involved in the enhanced blood clearance of a subsequent dose of PEGylated liposomes. J Control Release. 2007;119:236–44.
16. Ishida T, Ichihara M, Wang X, Kiwada H. Spleen plays an important role in the induction of accelerated blood clearance of PEGylated liposomes. J Control Release. 2006;115:243–50.
17. Ishida T, Wang X, Shimizu T, Nawata K, Kiwada H. PEGylated liposomes elicit an anti-PEG IgM response in a T cell-independent manner. J Control Release. 2007;122:349–55.
18. Ishida T, Kashima S, Kiwada H. The contribution of phagocytic activity of liver macrophages to the accelerated blood clearance (ABC) phenomenon of PEGylated liposomes in rats. J Control Release. 2008;126:162–5.
19. Caro J, Migliaccio-Walle K, Ishak KJ, Proskorovsky I. The morbidity and mortality following a diagnosis of peripheral arterial disease: long-term follow-up of a large database. BMC Cardiovasc Disord. 2005;5:14.
20. Chandra Sekhar N. Effect of eight prostaglandins on platelet aggregation. J Med Chem. 1970;13:39–44.
21. Simmet T, Peskar BA. Prostaglandin E1 and arterial occlusive disease: pharmacological considerations. Eur J Clin Invest. 1988;18:549–54.
22. Carlson LA, Olsson AG. Intravenous prostaglandin E1 in severe peripheral vascular disease. Lancet. 1976;2:810.
23. Belch JJ, Bell PR, Creissen D, Dormandy JA, Kester RC, McCollum RD, *et al.* Randomized, double-blind, placebo-controlled study evaluating the efficacy and safety of AS-013, a prostaglandin E1 prodrug, in patients with intermittent claudication. Circulation 1997;95:2298–302.
24. Ferreira SH, Vane JR. Prostaglandins: their disappearance from and release into the circulation. Nature 1967;216:868–73.
25. Golub M, Zia P, Matsuno M, Horton R. Metabolism of prostaglandins A1 and E1 in man. J Clin Invest. 1975;56:1404–10.
26. Monkhouse DC, Van Campen L, Aguiar AJ. Kinetics of dehydration and isomerization of prostaglandins E 1 and E 2. J Pharm Sci. 1973;62:576–80.
27. Mizushima Y, Yanagawa A, Hoshi K. Prostaglandin E1 is more effective, when incorporated in lipid microspheres, for treatment of peripheral vascular diseases in man. J Pharm Pharmacol. 1983;35:666–7.
28. Mizushima Y. Lipo-prostaglandin preparations. Prostaglandins Leukot Essent Fatty Acids. 1991;42:1–6.
29. Mizushima Y. Lipid microspheres as novel drug carriers. Drugs Exp Clin Res. 1985;11:595–600.
30. Mizushima Y, Hamano T, Haramoto S, Kiyokawa S, Yanagawa A, Nakura K, *et al.* Distribution of lipid microspheres incorporating prostaglandin E1 to vascular lesions. Prostaglandins Leukot Essent Fatty Acids. 1990;41:269–72.
31. Igarashi R, Mizushima Y, Takenaga M, Matsumoto K, Morizawa Y, Yasuda A. A stable PGE1 prodrug for targeting therapy. J Control Release. 1992;20:37–46.
32. Yoshida T, Uetake A, Yamaguchi H, Nimura N, Kinoshita T. New preparation method for 9-anthryldiazomethane (ADAM) as a fluorescent labeling reagent for fatty acids and derivatives. Anal Biochem. 1988;173:70–4.
33. Ishihara T, Takahashi M, Higaki M, Mizushima Y. Efficient encapsulation of a water-soluble corticosteroid in biodegradable nanoparticles. Int J Pharm. 2009;365:200–5.
34. Ishihara T, Izumo N, Higaki M, Shimada E, Hagi T, Mine L, *et al.* Role of zinc in formulation of PLGA/PLA nanoparticles encapsulating betamethasone phosphate and its release profile. J Control Release. 2005;105:68–76.
35. Bazile D, Prud'homme C, Bassoullet MT, Marlard M, Spenlehauer G, Veillard M. Stealth Me.PEG-PLA nanoparticles avoid uptake by the mononuclear phagocytes system. J Pharm Sci. 1995; 84:493–8.
36. Ishida T, Harada M, Wang XY, Ichihara M, Irimura K, Kiwada H. Accelerated blood clearance of PEGylated liposomes following preceding liposome injection: effects of lipid dose and PEG surface-density and chain length of the first-dose liposomes. J Control Release. 2005;105:305–17.
37. Lee SW, Chang DH, Shim MS, Kim BO, Kim SO, Seo MH. Ionically fixed polymeric nanoparticles as a novel drug carrier. Pharm Res. 2007;24:1508–16.

38. Musumeci T, Ventura CA, Giannone I, Ruozi B, Montenegro L, Pignatello R, *et al.* PLA/PLGA nanoparticles for sustained release of docetaxel. Int J Pharm. 2006;325:172–9.
39. Koide H, Asai T, Hatanaka K, Urakami T, Ishii T, Kenjo E, *et al.* Particle size-dependent triggering of accelerated blood clearance phenomenon. Int J Pharm. 2008;362:197–200.
40. Lu W, Wan J, She Z, Jiang X. Brain delivery property and accelerated blood clearance of cationic albumin conjugated pegylated nanoparticle. J Control Release. 2007;118:38–53.
41. Richter AW, Akerblom E. Polyethylene glycol reactive antibodies in man: titer distribution in allergic patients treated with monomethoxy polyethylene glycol modified allergens or placebo, and in healthy blood donors. Int Arch Allergy Appl Immunol. 1984;74:36–9.

Journal of Controlled Release 137 (2009) 234–240

Contents lists available at ScienceDirect

Journal of Controlled Release

journal homepage: www.elsevier.com/locate/jconrel

Effect of siRNA in PEG-coated siRNA-lipoplex on anti-PEG IgM production

Tatsuaki Tagami, Kazuya Nakamura, Taro Shimizu, Tatsuhiro Ishida, Hiroshi Kiwada *

Department of Pharmacokinetics and Biopharmaceutics, Subdivision of Biopharmaceutical Sciences, Institute of Health Biosciences, The University of Tokushima, 1-78-1, Sho-machi, Tokushima 770-8505, Japan

ARTICLE INFO

Article history:
Received 31 July 2008
Accepted 4 April 2009
Available online 8 April 2009

Keywords:
Accelerated blood clearance (ABC) phenomenon
Polyethylene glycol (PEG)
Anti-PEG IgM
PEG-coated siRNA/cationic liposome complex (PSCL)
Small interfering RNA (siRNA)

ABSTRACT

For efficient delivery of small interfering RNA (siRNA) *in vivo*, it is important to control the blood circulation of the delivery vehicle. Surface modification of the siRNA/cationic liposome complex (siRNA-lipoplex) with polyethylene glycol (PEG) is expected to enhance circulation time in blood. However, we have recently reported that anti-PEG IgM production after the first injection of PEG-coated liposome is responsible for a reduction in the blood circulation of the second dose of the liposome, which is known as the accelerated blood clearance (ABC) phenomenon. It is unknown whether a PEG-coated siRNA-lipoplex (PSCL) can cause the ABC phenomenon and anti-PEG IgM production. In this study, an anti-PEG IgM response to PSCL was detected and was inversely related to the PSCL dose. Interestingly, the anti-PEG IgM response was significantly lower for PSCL than it was for PEG-coated naked cationic liposomes (PCL). The studies with splenectomized mice and nude mice indicated that anti-PEG IgM production was closely related to an interaction of PSCL and PCL with the spleen, which is associated with a T cell-independent mechanism. In addition, PSCL induced apoptosis on IgM-expressing splenic cells more strongly than PCL did, which suggests that accumulation in the spleen and the apoptotic effect of PEG-coated substances on splenic B cells could affect the potency of anti-PEG IgM production.

© 2009 Elsevier B.V. All rights reserved.

1. Introduction

A small interfering RNA (siRNA) has sequence-specific and potent gene silencing properties based on an RNA interference mechanism for molecular-targeted drugs [1]. A growing number of studies have used siRNAs as potential therapeutic agents for treating numerous diseases, including cancer and genetic or viral infections [2,3]. The therapeutic application of siRNA is largely dependent on the development of a delivery vehicle and such a vehicle must be applied efficiently, safely and repeatedly. Cationic liposome is candidate that is expected to satisfy these requirements [4]. However, the use of a siRNA/cationic liposome complex (siRNA-lipoplex), such as systemic delivery in a clinical situation, is questionable due to poor blood circulation characteristics. Therefore, the surface of siRNA-lipoplex is frequently modified by polyethylene glycol (PEG)-conjugated lipid (PEGylation). PEGylation extends circulation time for liposomes, the mechanism of which is hypothesized to be as follows: the PEG on the liposomal surface attracts a water shell, resulting in the reduced adsorption of opsonins and the recognition of liposome by the cells of a mononuclear phagocyte system (MPS) [5,6]. The technology of PEG-coated liposomes is utilized for anti-cancer drugs in clinical settings [7]. The PEGylation of siRNA-lipoplexes may also enhance the circulation time of the complex and can increase the amount of siRNA in the targeted tissue, which offers significant potential for developing siRNA-based therapy, particularly for the application of systemic administration.

However, we and other researchers have reported that an intravenous injection of PEG-coated liposomes causes a second dose of PEG-coated liposomes, injected a few days later, to lose its long-circulating characteristics and to accumulate extensively in the liver [8,9], which is known as the "accelerated blood clearance (ABC) phenomenon." On the basis of our recent results [10,11], we proposed the following tentative mechanism for the cause of this phenomenon: anti-PEG IgM, which is produced in the spleen in response to a first dose, selectively binds to the PEG of the second dose liposomes injected several days later and subsequently activates the complement system. This, in turn, leads to opsonization of the second dose of liposome by C3 fragments and, as a consequence, to enhanced uptake of the liposomes by the Kupffer cells in the liver. In addition, we recently reported that the immune response to PEG on the liposome surface happens in a T cell-independent (TI) manner [12].

The ABC phenomenon involving anti-PEG IgM production can also be an important factor in designing an efficient delivery system of genes or nucleic acids. In an early study, it was reported that PEG-coated lipid nano-particles encapsulating plasmid DNA (pDNA) greatly enhances anti-PEG IgM production compared with PEG-coated nano-particles without pDNA. Consequently, pDNA expression declined highly in tumor tissue following its second injection [13].

* Corresponding author. Tel.: +81 88 633 7259; fax: +81 88 633 7260.
E-mail address: hkiwada@ph.tokushima-u.ac.jp (H. Kiwada).

0168-3659/$ – see front matter © 2009 Elsevier B.V. All rights reserved.
doi:10.1016/j.jconrel.2009.04.006

siRNA and pDNA also are well known as potent inducers of interferon and inflammatory cytokine when formulated with a lipid- or polycation-based delivery system [14,15]. For these reasons, we assumed that siRNA entrapped in PEG-coated cationic liposome affects the anti-PEG IgM response caused by the first dose of PSCL. In this study, therefore, we investigated the effect of siRNA in the PSCL on anti-PEG IgM production and the contribution of spleen and splenic B cells to the anti-PEG IgM responses caused by first PSCL dose.

2. Materials and methods

2.1. Materials

2-distearoyl-*sn*-glycero-3-phosphoethanolamine-*n*-[methoxy (polyethylene glycol)-2000 ($mPEG_{2000}$-DSPE), 1-palmitoyl-2-oleoyl-*sn*-glycero-3-phosphocholine (POPC) and dioleoylphospatidylethanolamine (DOPE) were generously donated by NOF (Tokyo, Japan). O,O′-ditetradecanoyl-N-(α-trimethyl ammonio acetyl) diethanolamine chloride (DC-6-14) as cationic lipid was purchased from Sogo Pharmaceutical (Tokyo, Japan). Cholesterol (CHOL) was of analytical grade (Wako Pure Chemical, Osaka, Japan). All lipids were used without further purification. ^{3}H-Cholesterylhexadecyl ether (^{3}H-CHE) was purchased from PerkinElmer Life Science (MA, USA). All other reagents were of analytical grade.

2.2. siRNA

siRNA, chemically synthesized and purified by HPLC, was purchased from Nippon EGT (Toyama, Japan). The sequence of siRNA for GFP, which does not have a target gene in mice, is as follows: sense sequence, 5′-GGC UAC GUC CAG GAG CGC ATT-3′; and, antisense sequence, 5′-UGC GCU CCU GGA CGU AGC CTT-3′. siRNA was dissolved in RNase free water at a final concentration of 50 μM.

2.3. Animals

Male Std-ddY mice aged 4–5 weeks (20–25 g), male BALB/cCr Slc mice aged 4–5 weeks (20–25 g), and male BALB/c Slc-nu/nu mice aged 5–6 weeks (20–25 g), were purchased from Japan SLC (Shizuoka, Japan). Mice were maintained under pathogen-free conditions. All animal experiments were evaluated and approved by the Animal and Ethics Review Committee of the University of Tokushima.

2.4. Preparation of cationic liposome

Cationic liposome was composed of DC-6-14:POPC:CHOL:DOPE (10:30:30:30, molar ratio). Liposome was prepared as previously described [12]. Briefly, the lipids were dissolved in chloroform. After evaporation of the organic solvent, the resulting lipid film was hydrated in 9% sucrose to produce multilamellar vesicles (MLVs). The MLVs were sized by repeated extrusion thorough polycarbonate membrane filters (Nucleopore, CA, USA) with consecutive pore size of 400, 200 and 100 nm. The mean diameters and zeta potentials of the resulting liposomes were determined using a NICOMP 370 HPL submicron particle analyzer (Particle Sizing System, CA, USA). The mean diameter and zeta potential for cationic liposome were 90.7 ± 2.3 nm and 18.5 ± 0.5 mV ($n = 3$), respectively. The lipid content of the liposomes was determined using a cholesterol E-test Wako kit (Wako Pure Chemical, Osaka, Japan).

2.5. Preparation of PEG-coated siRNA-lipoplex and PEG-coated cationic liposome

For the formulation of siRNA-lipoplex, for instance, siRNA (12.5 μg) and cationic liposome (0.625 μmol, phospholipids) were mixed and incubated for 20 min at room temperature. For PEGylation of siRNA-lipoplex and cationic liposome to produce PEG-coated siRNA-lipoplex (PSCL) and PEG-coated cationic liposome (PCL), a post-insertion technique was used [16]. Briefly, $mPEG_{2000}$-DSPE (5 mol% of total lipid) in 9% sucrose solution and siRNA-lipoplex or cationic liposome was mixed. The mixture was vortexed for 15 s and gently shaken for 1 h at 37 °C. The mean diameters were 205.4 ± 5.2 nm for PSCLs ($n = 3$) and 100.1 ± 3.9 nm for PCLs ($n = 3$). The mean zeta potentials were 9.0 ± 1.7 mV for PSCLs ($n = 3$) and 10.2 ± 1.2 mV for PCLs ($n = 3$). To check the presence of free siRNA in the prepared PSCL, electrophoresis was carried out with 2% Agarose gel. No bands relating free siRNA were detected, indicating that almost 100% of the siRNA was associated with and/or encapsulated in PEG-coated cationic liposome. In addition, to study RNase resistance of PSCL, PSCLs were incubated in 50% fetal bovine serum for 30 min at 37 °C. Then, the fragmentation of siRNA or released siRNA was determined using electrophoresis. No fragment of digested siRNA or released siRNA was detected. To determine the biodistribution of PCLs and PSCLs, the liposomes were labeled with a trace amount of ^{3}H-CHE (40 μCi/μmol of phospholipids) as a nonexchangeable lipid phase marker.

2.6. Splenic clearance of single injection

^{3}H-CHE labeled PSCL or ^{3}H-CHE labeled PCL (0.625 μmol phospholipids/mouse) were intravenously injected into mice via the tail vein. At selected post-injection time points (2 min, 15 min, 30 min, 1 h, 2 h, 4 h, 8 h or 24 h), the mice were euthanized. Blood samples were then obtained by heart puncture, and spleens were collected from the mice after withdrawing the blood samples. Radioactivity in spleen tissues was assayed as described previously [17]. Pharmacokinetic parameters were calculated using polyexponential curve fitting and the least-squares parameter estimation program SAAM II (Micromath, UT, USA).

The splenic clearance (CLs) was calculated as follows:

$$CLs = X_{(24)} / AUC_{(0\rightarrow 24)}.$$

Where $X_{(24)}$ (%Dose) is the amount of PSCLs or PCLs accumulated in spleen at 24 h post-injection. $AUC_{(0\rightarrow 24)}$ (%Dose·h/ml) is the area under the blood concentration-time curve from time 0 to 24 h post-injection.

2.7. Blood clearance and hepatic clearance of second injection (test liposome)

For pretreatment (first dose), either PSCL (0.625 μmol phospholipids and 12.5 μg siRNA/mouse) or PCL (0.625 μmol phospholipids/mouse) was intravenously injected into mice via the tail vein. To determine the biodistribution of the second dose, ^{3}H-CHE labeled PCL (test liposome, 0.625 μmol phospholipids/mouse) was intravenously injected into the mice via the tail vein at day 5 after the first injection. At selected post-injection time points (2 min, 15 min, 30 min, 1 h, 2 h, 4 h, 8 h or 24 h), the mice were euthanized. Blood samples were then obtained by heart puncture, and livers were collected from the mice after withdrawing the blood samples. Mice that were pretreated with 9% sucrose served as controls. Radioactivity in the blood and liver was assayed as described previously [17]. Pharmacokinetic parameters were calculated and the key parameters were obtained using polyexponential curve fitting and the least-squares parameter estimation program SAAM II.

The hepatic clearance (CLh) was calculated as follows:

$$CLh = X_{(24)} / AUC_{(0\rightarrow 24)}$$

Where $X_{(24)}$ (%Dose) is the amount of test liposomes accumulated in liver at 24 h post-injection. $AUC_{(0\rightarrow 24)}$ (%Dose·h/ml) is the area under the blood concentration-time curve from time 0 to 24 h post-injection.

2.8. Detection of IgM and IgG against PEG

A simple ELISA procedure as described before [12] was employed to detect IgM or IgG against PEG in the serum. Briefly, 10 nmol of $mPEG_{2000}$-DSPE in 50 μl ethanol was added to a 96-well plate. Lipid-coated plates were allowed to air dry completely for 2 h. The plates were then blocked for 1 h with Tris-buffered saline containing 1% BSA and were subsequently washed. Diluted serum samples (1:100) (100 μl) were then applied in appointed wells, incubated for 1 h and washed three times. Horseradish peroxidase (HRP)-conjugated antibody (100 μl, 1 μg/ml, Goat anti-mouse IgM (or IgG) IgG-HRP conjugate (Bethyl Laboratories, TX, USA)) was added to the wells. After incubation for 1 h, the wells were washed. ELISA activity was measured at 490 nm using a Microplate reader (Wallac1420 ARVOsx, PerkinElmer Life Science, MA, USA). All incubations were performed at room temperature.

2.9. Splenectomy

Splenectomy was carried out according to a method described earlier [10]. Briefly, after shaving the skin, a 2-cm incision was made in the skin of anaesthetized mice on the left flank. The peritoneal membrane was opened, and the entire spleen was removed after ligating the splenic vein and artery at the hilum. The peritoneal membrane and the skin were closed separately with surgical silk-thread. This procedure ensured that the spleen was removed in total and that no splenic fragments were left behind, as confirmed by examining the mice at the time of death. For sham-operated mice, the skin and peritoneal membrane were surgically opened and closed. One day (24 h) after surgery, either PSCLs or PCLs were injected into mice and blood samples were withdrawn on day 5 after injection. The detection of anti-PEG IgM in the sample was performed using ELISA, as described above.

2.10. Detection of apoptosis of IgM-expressing B cells in spleen

At 24 h post-injection of either PSCLs or PCLs, spleen tissues were removed from the mice under anaesthetization. As a positive control, an anti-cancer drug, doxorubicin solution (200 μg/mouse, approximately 8 mg/kg; Sigma, MO, USA), was intravenously injected. Spleen cell suspension was prepared using a Cell Strainer (100 μm, Becton Dickinson, NJ, USA) as described previously [12]. The apoptosis of splenic cells was detected using an "*in situ* cell death detection kit, Fluorescein" (Roche Diagnostics, Mannheim, Germany) according to the protocol manufacture recommended with minor modifications. To gate IgM-expressing B cells, cells were then incubated with Alexa Fluor 647 goat anti-mouse IgM (Invitrogen, CA, USA) for 1 h at room temperature. Cells were washed and then analyzed by flow cytometer (Guava EasyCyte Mini, GE Healthcare, CA, USA). In each sample, 30,000 cells were counted. Data analysis was performed using CytoSoft software (GE Healthcare).

2.11. Statistical analysis

All values are expressed as the mean ± S.D. Statistical analysis was performed with a two-tailed unpaired Student's *t* test using GraphPad InStat software (GraphPad Software, CA, USA). The level of significance was set at $p<0.05$.

3. Results

3.1. Dose dependency of PSCL or PCL on anti-PEG IgM production

We recently reported evidence indicating that anti-PEG IgM production after the first injection of PEG-coated empty liposome is responsible for the ABC phenomenon [11,12]. In the present study, to investigate the effect of siRNA in the PEG-coated siRNA lipoplex (PSCL) on anti-PEG IgM production, various doses of either PSCL or PCL were intravenously injected into mice. Anti-PEG IgM responses in serum were assessed on day 5 after the injection, which remarkably detected the induction of the ABC phenomenon, as in our previous report [11]. Anti-PEG IgM responses to PSCL and PCL showed a similar tendency (Fig. 1). Both anti-PEG IgM responses were reduced as their doses increased, and the responses were completely inhibited at higher dose (5 μmol phospholipids/mouse). Interestingly, at doses of 0.3125, 0.625 and 1.25 μmol phospholipids/mouse, anti-PEG IgM responses to PSCL were significantly lower than the responses to PCL.

To investigate whether the produced anti-PEG IgM accelerated clearance of the second dose, ^{3}H-CHE-labeled PCL (test liposome) was injected at day 5 after either PSCL (0.625 μmol phospholipids and 12.5 μg siRNA/mouse), PCL (0.625 μmol phospholipids/mouse) or 9% sucrose (control) was given. The blood concentration profile and calculated hepatic clearance (CLh) value are shown in Fig. 2. The test liposome showed a long-circulating characteristic in control mice ($T_{1/2}=12.4$ h) and a lower hepatic clearance value. In the mice pretreated with PCL, the test liposome cleared rapidly and completely disappeared from the blood within 24 h ($T_{1/2}=3.4$ h). Concomitantly, the CLh of test liposomes was increased by 10.2-fold compared with the control value. In the mice treated with PSCL, test liposome cleared rapidly from blood circulation, but the rate was moderate compared to that in the mice treated with PCL ($T_{1/2}=7.8$ h). Hepatic clearance was increased 4.6-fold compared to the control values.

3.2. Time course of changes in anti-PEG IgM or anti-PEG IgG responses

Then we investigated anti-PEG IgM and IgG responses as a function of time following injection with fixed doses (PSCL, 0.625 μmol phospholipids and 12.5 μg siRNA per mouse, approximately 25 μmol phospholipids and 500 μg siRNA per kg of body weight; PCL, 0.625 μmol phospholipids per mouse, approximately 25 μmol phospholipids per kg of body weight). As shown in Fig. 3, anti-PEG IgM responses were relatively higher than anti-PEG IgG responses, but a simultaneous tendency of anti-PEG IgM and anti-PEG IgG responses was generally observed the day after the injection of PSCL and PCL. Anti-PEG IgM and IgG responses were first detected at day 3 after the injection, reached the maximum at day 5, then decreased gradually

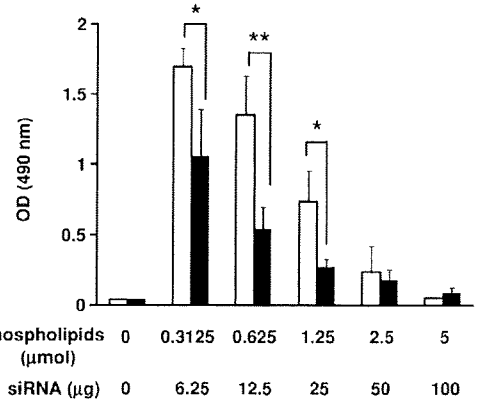

Fig. 1. Dose–response effect on the anti-PEG IgM response in mice. Various doses of either PSCL (0, 0.3125, 0.625, 1.25, 2.5 and 5 μmol phospholipids and 0, 6.25, 12.5, 25, 50 and 100 μg siRNA/mouse, respectively) or PCL (0, 0.3125, 0.625, 1.25, 2.5 and 5 μmol phospholipids/mouse) were intravenously injected into ddY mice. Five day later, blood was withdrawn and serum was collected. The sera collected from the naïve mice were used as the control (dose 0). Anti-PEG IgM was detected with ELISA as described in the Materials and methods section. □, PCL; ■, PSCL. Each value represents the mean ± S.D. ($n=4$). * $p<0.05$, ** $p<0.01$.

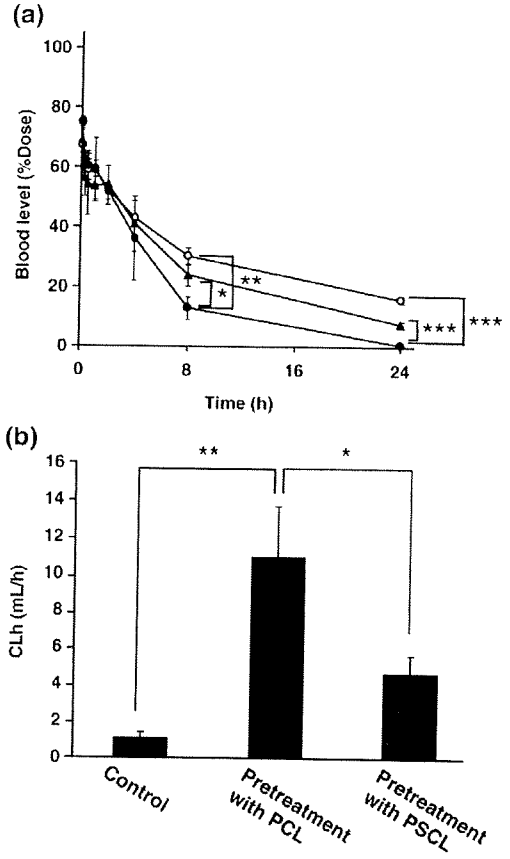

Fig. 2. Effect of the first dose of PSCL and PCL on blood clearance and hepatic clearance of the test dose of PCL, mice were pretreated with either PSCL (0.625 μmol phospholipids and 12.5 μg siRNA/mouse) or PCL (0.625 μmol phospholipids/mouse). Mice pretreated with 9% sucrose served as the control. At day 5 post-first injection, ^{3}H-CHE labeled PCL (test liposome, 0.625 μmol phospholipids/mouse) was intravenously injected. (a) Blood concentration profile of test liposome. ○, Control; ●, Mice pretreatment with PCL; ▲, Mice pretreatment with PSCL. (b) Hepatic clearance (CLh) of test liposome. Each value represents the mean ± S.D. ($n = 3$ or 4). * $p<0.05$, ** $p<0.01$, *** $p<0.005$.

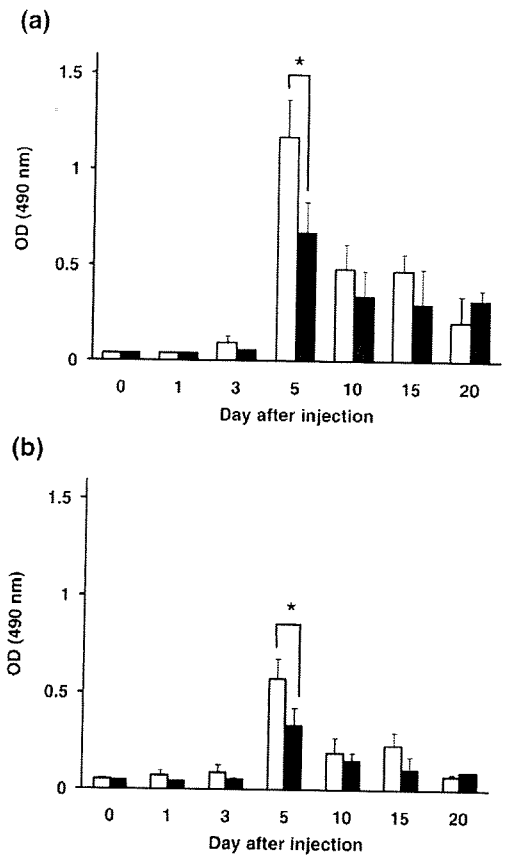

Fig. 3. Time course of changes in anti-PEG IgM and IgG response. Either PSCL (0.625 μmol phospholipids and 12.5 μg siRNA per mouse) or PCL (0.625 μmol phospholipids/mouse) were intravenously injected into the ddY mice. Blood was withdrawn and serum was collected 1–30 days after injection. The sera collected from the naïve mice were used as the control (Day 0). Anti-PEG IgM (a) and IgG (b) were detected using ELISA, as described in the Materials and methods section. □, PCL; ■, PSCL. Each value represents the mean ± S.D. ($n = 4$). * $p<0.05$.

but were persistently detected until day 20, which was the end point of the experiment. Anti-PEG IgM and anti-PEG IgG responses to PSCL were significantly lower than the responses to PCL at day 5 after the injection.

3.3. Anti-PEG IgM response in T cell-deficient (nude) mice

The peak day (day 5) for IgM and IgG responses observed in Fig. 3 was in accordance with a typical T cell-independent (TI) immune response [18]. To confirm whether anti-PEG IgM response to either PSCL or PCL was associated with the TI mechanism, PSCL or PCL was intravenously injected in T cell-deficient (nude) mice. As shown in Fig. 4, an anti-PEG IgM response was detected in both BALB/c nude mice and in BALB/c mice (Fig. 4). In addition, anti-PEG IgM response to PSCL was significantly lower than the response to PCLs in both types of mice ($p<0.05$).

3.4. Effect of splenectomy on anti-PEG IgM production

Our earlier study demonstrated that the spleen plays an important role in anti-PEG IgM production after PEG-coated empty liposome was intravenously administered [10]. Therefore, we investigated the contribution of the spleen to anti-PEG IgM production, induced by the intravenous injection of PSCL or PCL. In splenectomized mice, the anti-PEG IgM response to PSCL or PCL was almost attenuated to the control level (Fig. 5).

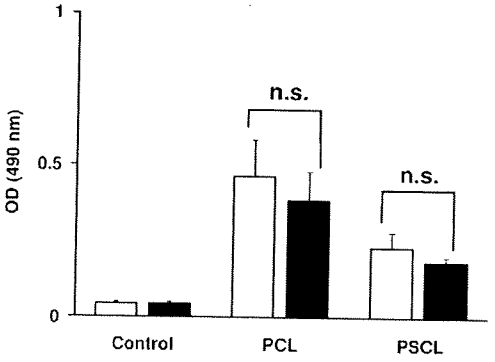

Fig. 4. Anti-PEG IgM responses in T cell-deficient (nude) mice. Either PSCL (0.625 μmol phospholipids and 12.5 μg siRNA/mouse) or PCL (0.625 μmol phospholipids/mouse) were intravenously injected into mice. Five days later, blood was withdrawn and serum was collected. The blood samples collected from the naïve mice were used as controls. Anti-PEG IgM was determined using ELISA, as described in the Materials and methods section. □, BALB/c mice; ■, BALB/c nude mice. Each value represents the mean ± S.D. ($n = 4$). n.s. means not significant.

GENE DELIVERY

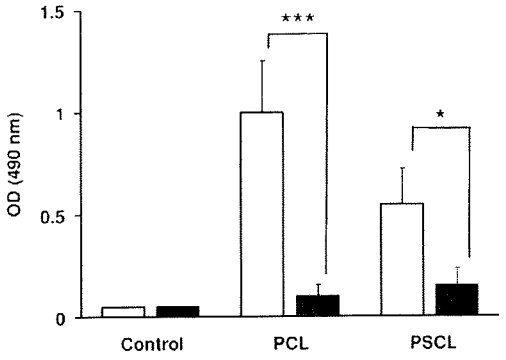

Fig. 5. Effect of splenectomy on anti-PEG IgM response. One day after splenectomy, either PSCL (0.625 μmol phospholipids and 12.5 μg siRNA/mouse) or PCL (0.625 μmol phospholipids/mouse) were intravenously injected into the ddY mice. Five days later, blood was withdrawn and serum was collected. The sera collected from the naïve mice were used as the control. Anti-PEG IgM was detected using ELISA, as described in the Materials and methods section. □, Control; ■, Splenectomy. Each value represents the mean ± S.D. ($n = 4$). * $p<0.05$, *** $p<0.005$.

3.5. Splenic clearance of the first dose of PSCL or PCL

The accumulation of either PSCL or PCL in the spleen was determined using either ^{3}H-CHE-labeled PSCL or ^{3}H-CHE-labeled PCL. PSCL showed a slight accumulation (approximately 5% dose/tissue) in the spleen, which was similar to PCL. In addition, splenic clearance (CLs) of PSCL and PCL was calculated (Fig. 6). The CLs of PSCL were higher than those of PCL, suggesting that splenic cells have a greater affinity for PSCL than for PCL, because CLs reflect the affinity of liposomes for the spleen [13].

3.6. The apoptotic effect of PSCL on IgM-expressing B cells in the spleen

The interaction of PSCL or PCL in the spleen, as observed in Fig. 6, might damage IgM-expressing B cells, which produce anti-PEG IgM. On day 5 after the injection, the damage (apoptosis) on IgM-expressing B cells in the spleen was evaluated using a flow cytometer. PSCL significantly induced apoptosis on IgM-expressing B cells (approximately 20% in the IgM-expressing B cells) compared with

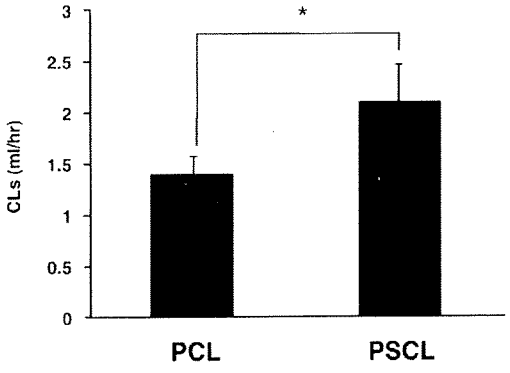

Fig. 6. Splenic clearance after a single intravenous injection of either PSCL or PCL in mice. ^{3}H-CHE labeled PSCL (0.625 μmol phospholipids and 12.5 μg siRNA/mouse) or ^{3}H-CHE labeled PCL (0.625 μmol phospholipids/mouse) were intravenously injected into ddY mice. At selected post-injection time points, blood samples and spleen were collected and radioactivity was measured. The calculation of splenic clearance is described in the Materials and methods section. Each value represents the mean ± S.D. ($n = 3$ or 4). * $p<0.05$.

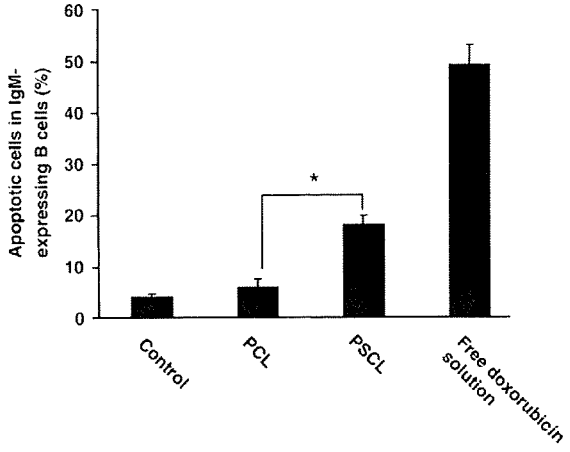

Fig. 7. Apoptotic effect of either PSCL or PCL on IgM-expressing B cells in the spleen. Either PSCL (0.625 μmol phospholipids and 12.5 μg siRNA/mouse) or PCL (0.625 μmol phospholipids/mouse) were intravenously injected into ddY mice. As a positive control, doxorubicin solution (8 mg/kg) was intravenously injected into mice. At 24 h after injection, the splenic cells were collected and treated with "the *in situ* cell death detection kit." IgM-expressing B cells in the splenic cells were gated following staining with anti-mouse IgM antibody. Then the apoptosis of B cells gated were analyzed by flow cytometer. Each value represents the mean ± S.D. ($n = 5$). * $p<0.05$.

that of PCL (Fig. 7). On the other hand, PCL showed no apoptotic effect on IgM-expressing B cells.

4. Discussion

The key success factor for siRNA-based therapy has been summarized in the efficacy of the siRNA delivery system [2,3]. The PEG-coated delivery vehicle was endowed with an enormous advantage in the prolonging of blood circulation time for siRNA, but anti-PEG IgM production, would cause the ABC phenomenon, consequently reducing the resident time of siRNA in blood circulation. In this study, we tried to investigate the effect of siRNA in the PEG-coated siRNA-lipoplex (PSCL) on anti-PEG IgM production. Herein, we confirmed that the intravenous injection of both PSCL and PCL induces anti-PEG IgM production (Fig. 1) and consequently causes a second dose of test PCL, injected 5 days later, to lose its long-circulating characteristics and accumulate extensively in the liver (Fig. 2). To the best of our knowledge, this is the first report of anti-PEG IgM production causing the ABC phenomenon by intravenous administration of a PEG-coated vehicle containing siRNA.

In the present study, we found that anti-PEG IgM production was reduced as injected doses were increased (Fig. 1). Such an inverse relationship had already been observed in our previous report using empty PEG-coated neutral liposome in rats [19]. The higher dose might lead the B cells to become inactivated or apoptotic, as described in Fig. 7, and thus inhibit the anti-PEG IgM production. Furthermore, it is noted that the induction of the ABC phenomenon could be prevented by a higher dose of either PSCL or PCL, because the anti-PEG IgM production was completely inhibited by the higher dose (100 μg siRNA and/or 5 μmol, phospholipids/mouse) (Fig. 1). Recent research has shown the successful *in vivo* therapeutic effect of siRNA when preferentially used at a higher dose (100 μg/mouse or more) either with or without PEGylation as a delivery vehicle [2,3]. Such higher doses might be one of the reasons that significant *in vivo* therapeutic effects were achieved with repeated administration. However, minimizing the dosage of siRNA is required for clinical use, since siRNA is still expensive. Hence, ant-PEG IgM production, and the resultant the ABC phenomenon, may emerge as one of essential problems in the use of a PEG-coated vehicle for siRNA delivery.

Splenectomy (removal of the spleen from a mouse) significantly inhibited the production of anti-PEG IgM from pretreatment with

PSCL and PCL (Fig. 5). This suggests that the spleen plays an important role in the immune response to PSCL and PCL. In addition, naïve mice and nude mice, which lack T cells, produced anti-PEG IgM in a similar manner (Fig. 4), suggesting that the immune response against PSCL and PCL in mice is derived in a T cell independent manner. This concern is supported by observations from the time course study on anti-PEG IgM and anti-PEG IgG (Fig. 3). The peak day for anti-PEG IgM and anti-PEG IgG production was in accordance with that of a typical T cell independent immune response [18]. Recently, a similar T cell independent immune response was reported in mice immunized with CpG ODN-containing PEG-coated liposome [20] and ODN-containing PEG-coated liposomes [21].

Our earlier [10,12] and current results strongly indicate that splenic B cells play an important role in the production of anti-PEG IgM in a T cell independent manner. In a general T cell independent immune response, B cells are well known to be activated and produce antibodies by themselves [22,23]. The splenic clearance of PSCL was higher than that of PCL (Fig. 6), although the accumulation amount of PSCL in the spleen was similar to that of PCL (approx. 5% dose/tissue). This suggests that PSCL has a much higher affinity to spleen cells than PCL does, and, therefore, has more chance to interact with splenic B cells. The higher affinity of PSCL than PCL might be due to a difference in surface physicochemical properties of the prepared lipoplexes, between PSCL and PCL. But, due to a lack of basic studies concerning the effect of siRNA on the cationic liposome/lipids in biodistribution, the mechanism of the interaction remains unclear. The greater accessibility of PSCL in comparison with PCL (Fig. 6) might promote more apoptosis in IgM expressing splenic B cells (Fig. 7). Recently, it was reported that siRNA could non-specifically activate cells of the immune system, including the IFN system, and induce the production of cytokines and apoptosis both *in vitro* and *in vivo* [13,24–30]. Moreover, we and other groups have reported *in vitro* studies finding that the expression level of several endogenous genes related to cytokines and apoptosis was enhanced by siRNA transfected by non-viral vectors, Lipofectamine 2000 [31,32] and Oligofectamine [33]. Therefore, we now assume that apoptosis in IgM-expressing B cells could be one of the consequences of non-specific cellular immune responses on IgM-expressing cells and/or splenocytes induced by PSCL, although the precise mechanism remains unclear.

The cell damage by PSCL, observed in Fig. 7, might affect the moderation of anti-PEG IgM production, resulting in different anti-PEG IgM production (Fig. 1) and different ABC phenomenon induction (Fig. 2). Latinne et al. [34] reported that doxorubicin induced apoptosis of B cells and consequently depleted them. We also recently reported that the injection of doxorubicin containing PEG-coated liposome as the first dose dramatically reduced anti-PEG IgM production and consequently diminished the ABC phenomenon [35]. These reports support the theory that the reduction of anti-PEG IgM production may result from apoptosis and inactivation of splenic B cells, although the precise mechanism must be elucidated.

In the early studies, other groups have reported that pDNA and ODN encapsulated in PEG-coated nano-particles greatly enhanced anti-PEG IgM production [13,21]. It is known that nonmethylated bacterial DNA and synthetic ODN can stimulate mononuclear cells and lymphocytes both *in vitro* and *in vivo*, resulting in the secretion of IL6, IL12 and IgM [36]. Hence, the enhancement effect is likely to be attributed to CpG motifs and the palindromic sequence motif. Recent studies indicate that siRNAs, which have specific sequences such as GU-rich, can be potent activators of an innate immune response [24,37,38]. Since siRNA is reportedly recognized by Toll-like receptor-3, -7 and -8 [39], such siRNAs, which have immune stimulatory sequences, may greatly stimulate Toll-like receptors which are expressed in IgM-expressing B cells, and consequently indirectly affect the anti-PEG IgM production induced by the PEG-coated siRNA-lipoplex. The strength of the stimulatory effect on anti-PEG IgM production may be different among siRNA, ODN and pDNA in a sequence-dependent manner. In fact, Li et al. [40] recently reported that PEG-coated lipid nano-particles encapsulated with pDNA significantly induced the secretion of inflammatory cytokines such as IL-6, IL-12 and INF-γ compared to those encapsulated with siRNA.

Nevertheless, the precise mechanism by which PSCL produces anti-PEG IgM and attenuates IgM production remains unknown (Fig. 1). The results of the present study suggest that anti-PEG IgM production is strongly related to the interaction of PSCL with splenic IgM-expressing B cells. Hence, further precise study is required for information that will improve the efficacy of the siRNA delivery system.

5. Conclusion

Our study has significant implications for the use of PEG-coated cationic liposome in the therapeutic evaluation of siRNA drugs. Nonviral, lipid-based delivery systems are generally thought to be nonimmunogenic. PEGylation is expected to attenuate immunogenicity of the carrier components. However, we demonstrated that either PSCL or PCL will activate the immune system, resulting in the production of anti-PEG IgM. Our study presented herein indicates that PEG-coated cationic liposome must be used with caution for applications involving siRNA-based therapeutics, and these results increase the importance of evaluating carrier-directed effects of siRNA-based delivery system.

Acknowledgements

We thank Dr. James L. McDonald for his helpful advice in writing the English manuscript. This work was supported in part by the Health and Labour Sciences Research Grants for Research on Advanced Medical Technology from the Ministry of Health, Labour and Welfare of Japan, and by a Grant-in-Aid for Scientific Research on Priority Areas Cancer, Ministry of Education, Culture, Sports and Technology (20015033).

References

[1] S.M. Elbashir, J. Harborth, W. Lendeckel, A. Yalcin, K. Weber, T. Tuschl, Duplexes of 21-nucleotide RNAs mediate RNA interference in cultured mammalian cells, Nature 411 (2001) 494–498.
[2] S. Akhtar, I.F. Benter, Nonviral delivery of synthetic siRNAs in vivo, J. Clin. Invest. 117 (2007) 3623–3632.
[3] M.A. Behlke, Progress towards in vivo use of siRNAs, Molec. Ther. 13 (2006) 644–670.
[4] P.L. Felgner, T.R. Gadek, M. Holm, R. Roman, H.W. Chan, M. Wenz, J.P. Northrop, G.M. Ringold, M. Danielsen, Lipofection: a highly efficient, lipid-mediated DNA-transfection procedure, Proc. Natl. Acad. Sci. U. S. A. 84 (1987) 7413–7417.
[5] D. Papahadjopoulos, T.M. Allen, A. Gabizon, E. Mayhew, K. Matthay, S.K. Huang, K.D. Lee, M.C. Woodle, D.D. Lasic, C. Redemann, et al., Sterically stabilized liposomes: improvements in pharmacokinetics and antitumor therapeutic efficacy, Proc. Natl. Acad. Sci. U. S. A. 88 (1991) 11460–11464.
[6] V.P. Torchilin, V.G. Omelyanenko, M.I. Papisov, A.A. Bogdanov Jr., V.S. Trubetskoy, J.N. Herron, C.A. Gentry, Poly (ethylene glycol) on the liposome surface: on the mechanism of polymer-coated liposome longevity, Biochim. Biophys. Acta 1195 (1994) 11–20.
[7] Z. Symon, A. Peyser, D. Tzemach, O. Lyass, E. Sucher, E. Shezen, A. Gabizon, Selective delivery of doxorubicin to patients with breast carcinoma metastases by stealth liposomes, Cancer 86 (1999) 72–78.
[8] E.T. Dams, P. Laverman, W.J. Oyen, G. Storm, G.L. Scherphof, J.W. van Der Meer, F.H. Corstens, O.C. Boerman, Accelerated blood clearance and altered biodistribution of repeated injections of sterically stabilized liposomes, J. Pharmacol. Exp. Ther. 292 (2000) 1071–1079.
[9] T. Ishida, H. Kiwada, Accelerated blood clearance (ABC) phenomenon upon repeated injection of PEGylated liposomes, Int. J. Pharm. 354 (2008) 56–62.
[10] T. Ishida, M. Ichihara, X. Wang, H. Kiwada, Spleen plays an important role in the induction of accelerated blood clearance of PEGylated liposomes, J. Control. Release 115 (2006) 243–250.
[11] T. Ishida, M. Ichihara, X. Wang, K. Yamamoto, J. Kimura, E. Majima, H. Kiwada, Injection of PEGylated liposomes in rats elicits PEG-specific IgM, which is responsible for rapid elimination of a second dose of PEGylated liposomes, J. Control. Release 112 (2006) 15–25.
[12] T. Ishida, X. Wang, T. Shimizu, K. Nawata, H. Kiwada, PEGylated liposomes elicit an anti-PEG IgM response in a T cell-independent manner, J. Control. Release 122 (2007) 349–355.
[13] A. Judge, K. McClintock, J.R. Phelps, I. Maclachlan, Hypersensitivity and loss of disease site targeting caused by antibody responses to PEGylated liposomes, Molec. Ther. 13 (2006) 328–337.

[14] Z. Ma, J. Li, F. He, A. Wilson, B. Pitt, S. Li, Cationic lipids enhance siRNA-mediated interferon response in mice, Biochem. Biophys. Res. Commun. 330 (2005) 755–759.
[15] M. Sioud, D.R. Sorensen, Cationic liposome-mediated delivery of siRNAs in adult mice, Biochem. Biophys. Res. Commun. 312 (2003) 1220–1225.
[16] T.M. Allen, P. Sapra, E. Moase, Use of the post-insertion method for the formation of ligand-coupled liposomes, Cell. Mol. Biol. Lett. 7 (2002) 889–894.
[17] H. Harashima, C. Yamane, Y. Kume, H. Kiwada, Kinetic analysis of AUC-dependent saturable clearance of liposomes: mathematical description of AUC dependency, J. Pharmacokinet. Biopharm. 21 (1993) 299–308.
[18] A. Zandvoort, W. Timens, The dual function of the splenic marginal zone: essential for initiation of anti-TI-2 responses but also vital in the general first-line defense against blood-borne antigens, Clin. Exp. Immunol. 130 (2002) 4–11.
[19] T. Ishida, M. Harada, X. Wang, M. Ichihara, K. Irimura, H. Kiwada, Accelerated blood clearance of PEGylated liposomes following preceding liposome injection: effects of lipid dose and PEG surface-density and chain length of the first-dose liposomes, J. Control. Release 105 (2005) 305–317.
[20] W.M. Li, M.B. Bally, M.P. Schutze-Redelmeier, Enhanced immune response to T-independent antigen by using CpG ologodeoxynucleotides encapsulated in liposomes, Vaccine 20 (2001) 148–157.
[21] S.C. Semple, T.O. Harasym, K.A. Clow, S.M. Ansell, S.K. Klimuk, M.J. Hope, Immunogenicity and rapid blood clearance of liposomes containing polyethylene glycol-lipid conjugates and nucleic Acid, J. Pharmacol. Exp. Ther. 312 (2005) 1020–1026.
[22] J.J. Mond, A. Lees, C.M. Snapper, T cell-independent antigens type 2, Annu. Rev. Immunol. 13 (1995) 655–692.
[23] Q. Vos, A. Lees, Z.Q. Wu, C.M. Snapper, J.J. Mond, B-cell activation by T-cell-independent type 2 antigens as an integral part of the humoral immune response to pathogenic microorganisms, Immunol. Rev. 176 (2000) 154–170.
[24] A.D. Judge, V. Sood, J.R. Shaw, D. Fang, K. McClintock, I. MacLachlan, Sequence-dependent stimulation of the mammalian innate immune response by synthetic siRNA, Nat. Biotechnol. 23 (2005) 457–462.
[25] J.T. Marquesand, B.R. Williams, Activation of the mammalian immune system by siRNAs, Nat. Biotechnol. 23 (2005) 1399–1405.
[26] C.A. Sledz, M. Holko, M.J. de Veer, R.H. Silverman, B.R. Williams, Activation of the interferon system by short-interfering RNAs, Nat. Cell Biol. 5 (2003) 834–839.
[27] K. Kariko, P. Bhuyan, J. Capodici, D. Weissman, Small interfering RNAs mediate sequence-independent gene suppression and induce immune activation by signaling through toll-like receptor 3, J. Immunol. 172 (2004) 6545–6549.
[28] S.P. Persengiev, X. Zhu, M.R. Green, Nonspecific, concentration-dependent stimulation and repression of mammalian gene expression by small interfering RNAs (siRNAs), RNA 10 (2004) 12–18.
[29] A. Judge, I. MacLachlan, Overcoming the innate immune response to small interfering RNA, Hum. Gene Ther. 19 (2008) 111–124.
[30] S. Spagnou, A.D. Miller, M. Keller, Lipidic carriers of siRNA: differences in the formulation, cellular uptake, and delivery with plasmid DNA, Biochemistry 43 (2004) 13348–13356.
[31] M.A. Robbins, M. Li, I. Leung, H. Li, D.V. Boyer, Y. Song, M.A. Behlke, J.J. Rossi, Stable expression of shRNAs in human CD34+ progenitor cells can avoid induction of interferon responses to siRNAs in vitro, Nat. Biotechnol. 24 (2006) 566–571.
[32] T. Tagami, K. Hirose, J.M. Barichello, T. Ishida, T.H. Kiwada, Global gene expression profiling in cultured cells is strongly influenced by treatment with siRNA-cationic liposome complexes, Pharm. Res. 25 (2008) 2497–2504.
[33] J.T. Marques, T. Devosse, D. Wang, M. Zamanian-Daryoush, P. Serbinowski, R. Hartmann, T. Fujita, M.A. Behlke, B.R. Williams, A structural basis for discriminating between self and nonself double-stranded RNAs in mammalian cells, Nat. Biotechnol. 24 (2006) 559–565.
[34] D. Latinne, M. Soares, X. Havaux, F. Cormont, B. Lesnikoski, F.H. Bach, H. Bazin, Depletion of IgM xenoreactive natural antibodies by injection of anti-mu monoclonal antibodies, Immunol. Rev. 141 (1994) 95–125.
[35] T. Ishida, K. Atobe, X. Wang, H. Kiwada, Accelerated blood clearance of PEGylated liposomes upon repeated injections: effect of doxorubicin-encapsulation and high-dose first injection, J. Control. Release 115 (2006) 251–258.
[36] A.M. Krieg, CpG motifs in bacterial DNA and their immune effects, Annu. Rev. Immunol. 20 (2002) 709–760.
[37] M. Sioud, Induction of inflammatory cytokines and interferon responses by double-stranded and single-stranded siRNAs is sequence-dependent and requires endosomal localization, J. Mol. Biol. 348 (2005) 1079–1090.
[38] V. Patzel, In silico selection of active siRNA, Drug Discov. Today 12 (2007) 139–148.
[39] M. Sioud, RNA interference and innate immunity, Adv. Drug Deliv. Rev. 59 (2007) 153–163.
[40] S.D. Li, Y.C. Chen, M.J. Hackett, L. Huang, Tumor-targeted delivery of siRNA by self-assembled nanoparticles, Molec. Ther. 16 (2008) 163–169.

Journal of Controlled Release 137 (2009) 8–14

Contents lists available at ScienceDirect

Journal of Controlled Release

journal homepage: www.elsevier.com/locate/jconrel

Oxaliplatin encapsulated in PEG-coated cationic liposomes induces significant tumor growth suppression via a dual-targeting approach in a murine solid tumor model

Amr S. Abu Lila, Shinji Kizuki, Yusuke Doi, Takuya Suzuki, Tatsuhiro Ishida *, Hiroshi Kiwada

Department of Pharmacokinetics and Biopharmaceutics, Subdivision of Biopharmaceutical Sciences, Institute of Health Biosciences, The University of Tokushima, 1-78-1, Sho-machi, Tokushima 770-8505, Japan

ARTICLE INFO

Article history:
Received 15 January 2009
Accepted 27 February 2009
Available online 12 March 2009

Keywords:
Anticancer therapy
Drug delivery system
Anticancer drug
Oxaliplatin
PEG-coated cationic liposomes

ABSTRACT

We recently designed a PEG-coated cationic liposome targeted to angiogenic vessels and showed, in a murine dorsal air sac model, potent anti-angiogenic activity of an oxaliplatin (l-OHP) formulation of this liposome. In the present study, we extended the l-OHP formulation to a murine tumor-xenograft model. Following three injections, l-OHP containing PEG-coated cationic liposomes showed substantial tumor growth suppression and increased survival time of tumor-bearing mice without apparent side effects, compared with other l-OHP containing PEG-coated neutral liposomes and free l-OHP. In vivo imaging showed a preferential tumor accumulation and a broader distribution of PEG-coated cationic liposomes, compared with PEG-coated neutral liposomes. In addition, PEG-coated cationic liposomes delivered larger amounts of l-OHP into the tumor tissue than other l-OHP formulations, correlating with its antitumor efficiency. In vitro studies indicated that PEG-coated cationic liposomes were internalized not only by tumor cells but also by endothelial cells, and consequently its l-OHP formulation displayed higher cytotoxicity towards both cell types as compared with l-OHP containing PEG-coated neutral liposomes. In summary, l-OHP containing PEG-coated cationic liposomes induced significant tumor growth suppression, presumably by delivering encapsulated l-OHP into both tumor endothelial cells and tumor cells. Such dual targeting approach, i.e. vascular-targeting and tumor-targeting with a single liposomal l-OHP formulation, may have great potential for overcoming some major limitations in conventional chemotherapy.

© 2009 Elsevier B.V. All rights reserved.

1. Introduction

Oxaliplatin (l-OHP), a cisplatin derivative, has been approved for standard first- and second-line treatment of metastatic or advanced-stage colorectal cancer in combination with the infusion of 5-fluorouracil (5-FU)/leucovorin (FOLFOX) [1–3]. However, when used alone, its clinical efficiency is limited by the dose-limiting side effects such as neurotoxicity [4–6] and by high partitioning to erythrocytes in vivo [6]. Substantial efforts have been dedicated to solve these problems. One of the most intriguing strategies to overcome these drawbacks is to encapsulate l-OHP in a targetable drug delivery system such as liposomes [7–9].

Recently, we designed a polyethylene glycol (PEG)-coated cationic liposome to target the newly formed angiogenic vessels and developed a l-OHP formulation based on these liposomes. This targeted liposomal l-OHP formulation showed a remarkable in vivo anti-angiogenic activity in a mouse dorsal air sac (DAS) model [10]. Cationic liposomes have been reported to display a strong binding ability to tumor-derived angiogenic vascular endothelial cells and tumor cells due to the strong electrostatic adhesion between the cationic surface and the plasma membrane of cells [11–13]. In addition, grafting of PEG to the surface of the liposome may extend the circulation lifetime of the cationic liposome by preventing interactions with the biological in vivo environment [14–16]. This results in extensive extravasation of the liposomes due to the tumor-selective enhanced permeability and retention (EPR) effect [17], ultimately leading to enhanced accumulation of the liposomes in the tumor interstitium. We hypothesized that the specific properties of our PEG-coated cationic liposomes might enhance their chance to gain access not only to the endothelial cells in the originally targeted angiogenic vessels but also to the tumor cells following extravasation into the interstitial space. Hence, we assumed that, by our dual targeting approach to both endothelial cells in angiogenic vessels and

Abbreviations: CHOL, cholesterol; DC-6-14, O,O′-ditetradecanoyl-N-(alpha trimethyl ammonioacetyl)diethanolamine chloride; DiI, 1,1′-dioctadecyl-3,3,3′,3′-tetramethylindocarbocyanine perchlorate; DMEM, Dulbecco's modified Eagle's medium; EDTA, ethylenediamine tetraacetic acid; EGF, epidermal growth factor; FBS, fetal bovine serum; FCS, fetal calf serum; 5FU, 5-flourouracil; GA, gentamicin sulfate; HSPC, hydrogenated soya phosphatidylcholine; HUVEC, Human umbilical vascular endothelial cells; IGF-1, insulin-like growth factor; LLCC, Lewis lung carcinoma cells; l-OHP, oxaliplatin; $mPEG_{2000}$-DSPE, 1,2-distearoyl-sn-glycero-3-phosphoethanolamine-*n*-[methoxy (polyethyleneglycol)-2000]; MTT, 3-(4,5-dimethylthiazol-2-yl)-2,5 diphenyl tetrazolium bromide; PBS, Phosphate buffered saline; Pt, platinum; VEGF, vascular endothelial growth factor.

* Corresponding author. Tel./fax: +81 88 633 7260.
E-mail address: ishida@ph.tokushima-u.ac.jp (T. Ishida).

0168-3659/$ – see front matter © 2009 Elsevier B.V. All rights reserved.
doi:10.1016/j.jconrel.2009.02.023

tumor cells [18,19], l-OHP containing PEG-coated cationic liposomes will show markedly enhanced antitumor activity, as compared to l-OHP containing PEG-coated neutral liposomes (conventional PEG-coated liposomes).

In this study, we therefore investigated the therapeutic activity of l-OHP containing PEG-coated cationic liposomes in an in vivo murine solid tumor model. In addition, we evaluated the potential of the liposomes to extend the delivery of adequate quantities of l-OHP to tumors in vivo and to kill both tumor cells (Lewis lung carcinoma cells (LLCC)) and human umbilical vascular endothelial cells (HUVEC) in vitro.

2. Materials and methods

2.1. Materials

Hydrogenated soy phosphatidylcholine (HSPC) and 1,2-distearoyl-sn-glycero-3-phosphoethanolamine-*n*-[methoxy (polyethyleneglycol)-2000] ($mPEG_{2000}$-DSPE) were generously donated by NOF (Tokyo, Japan). Oxaliplatin (l-OHP) was generously donated by Taiho Pharmaceutical (Tokyo, Japan). Cholesterol (CHOL) and O,O′-ditetradecanoyl-N-(alpha-trimethyl ammonio acetyl) diethanolamine chloride (DC-6-14) were purchased from Sogo Pharmaceutical (Tokyo, Japan). 1,1′-dioctadecyl-3,3,3′,3′-tetramethyl-indocarbocyanine perchlorate (DiI) was purchased from Invitrogen (OR, USA). 3-(4,5-dimethylthiazol-2-yl)-2,5-diphenyltetrazolium bromide (MTT) was purchased from Nacalai Tesque (Kyoto, Japan). All other reagents were of analytical grade.

2.2. Animals and tumor cell line

Male C57BL/6 mice, 4 weeks old, were purchased from Japan SLC (Shizuoka, Japan). The experimental animals were allowed free access to water and mouse chow, and were housed under controlled environmental conditions (constant temperature, humidity, and 12 h dark–light cycle). All animal experiments were evaluated and approved by the Animal and Ethics Review Committee of the University of Tokushima. Lewis lung carcinoma cell (LLCC) line was purchased from Cell Resource Center for Biomedical Research (Institute of Development, Aging and Cancer, Tohoku University). LLCC line was maintained in Dulbecco's modified Eagle's medium (DMEM) (Nissui Pharmaceutical Co. Ltd., Tokyo, Japan) supplemented with 10% heat-inactivated FBS (Japan Bioserum, Hiroshima, Japan), 10 mM L-glutamine, 100 U/ml penicillin and 100 μg/ml streptomycin in a 5% CO_2/air incubator at 37 °C. Human umbilical vascular endothelial cells (HUVEC) were maintained in EBM-2 medium (Cambrex Bioscience, Walkersville, MD, USA) containing 10% fetal calf serum (FCS), vascular endothelial growth factor (VEGF), insulin-like growth factor (IGF-1), ascorbic acid, epidermal growth factor (EGF), GA-100 and heparin.

2.3. Preparation of liposomes

Cationic liposomes modified with $mPEG_{2000}$-DSPE were composed of HSPC/CHOL/DC-6-14/$mPEG_{2000}$-DSPE (2/1/0.2/0.2 molar ratio). Neutral liposomes modified with $mPEG_{2000}$-DSPE were composed of HSPC/CHOL/$mPEG_{2000}$-DSPE (2/1/0.2 molar ratio). For cellular uptake experiments and in vivo imaging experiments, 1 mol% of the fluorescent dye DiI was incorporated in the lipid mixture. All liposomes were prepared according to the method described earlier [10]. Briefly, lipids (50 mmol) were dissolved in 6 ml of chloroform/diethyl ether (1:2 v/v) and then 2 ml of l-OHP solution (8 mg/ml) in 5% (w/v) dextrose was dropped into the lipid mixture to form a w/o emulsion. For preparation of empty PEG-coated cationic liposomes, 5% dextrose solution was added instead of l-OHP solution. The volume ratio of the aqueous to the organic phase was maintained at 1:3. The emulsion was sonicated for 15 min and then the organic phase was removed to form liposomes by evaporation in a rotary evaporator at 40 °C under reduced pressure at 250 hPa for 1 h. The resulting liposomes were extruded through a polycarbonate membrane (200 nm pore size) using an extruder device (Lipex Biomembranes Inc., Vancouver, Canada) maintained at 65 °C to obtain liposomes with approximately 200 nm in a mean diameter. The phospholipid concentration was determined by colorimetric assay [20]. Un-encapsulated, free l-OHP was removed by dialysis by means of a dialysis cassette (Slyde-A-Lyzer, 10000MWCO, PIERCE, IL, USA) against 5% dextrose. Encapsulated l-OHP was quantified using an atomic absorption photometer (Z-5700, Hitachi, Tokyo, Japan). The size and zeta potential of the liposomes were determined by using a NICOMP 370 HPL submicron particle analyzer (Particle Sizing System, CA, USA). The encapsulation efficiency of l-OHP was calculated by dividing the drug to lipid ratio after the dialysis by the initial drug to lipid ratio. The encapsulation efficiency was approximately 20% in both liposomes. These values are three times higher than that reported recently by other group [7]. The physicochemical properties and encapsulation efficiency of the liposome preparations are summarized in Table 1.

2.4. Cellular uptake experiments

2.4.1. Cellular uptake of DiI-labeled liposomes

LLCC (2.5×10^4) were seeded onto 12-well plates in 1 ml of DMEM containing 10% FBS and pre-incubated for 24 h. HUVEC (2.5×10^4) were also seeded onto 12-well plates in 1 ml EBM-2 medium containing 10% serum for 24 h. After removal of culture medium, 1 ml of fresh medium containing either DiI-labeled PEG-coated neutral or cationic liposomes (4 μmol of lipids/well) was added, followed by incubation at 37 °C. At 4, 8, 12 and 24 h post-incubation, the cells were trypsinized following a single washing with cold phosphate buffered saline (PBS, 37 mM NaCl, 2.7 mM KCl, 8.1 mM Na_2HPO_4 and 1.47 mM KH_2PO_4; pH 7.4). The cells were collected into a 1.5 ml-Eppendorf tube and then treated for 5 min at room temperature with 0.3% trypan blue to quench extracellular fluorescence [21], followed by washing twice with PBS. This step is necessary in order to differentiate between membrane-bound and internalized liposomes. The cells were re-suspended in 200 μl of PBS containing 0.5 mM EDTA (EDTA-PBS). The cellular uptake of DiI-labeled liposomes was quantified using a flow cytometer with a Guava EastCyte™ MiniSystem (Guava Technologies, CA, USA) equipped with an argon-ion laser and 560 nm band pass filters for emission measurements. Approximately 10,000 events were acquired per sample, and the data were analyzed using Guava Express Plus software.

2.4.2. Uptake mechanism

To investigate the mechanism of internalization of DiI-labeled PEG-coated cationic liposome, LLCC (2.5×10^4) were seeded onto 24-well plates in 1 ml DMEM containing 10% FBS for 24 h.

HUVEC (2.5×10^4) were also seeded onto 24-well plates in 1 ml EBM-2 medium containing 10% FCS for 24 h. After pre-incubation, the culture medium was removed and the cells were further incubated for 30 min in the absence or presence of one of the following uptake inhibitors: sucrose (0.45 M) to inhibit formation of clathrin-coated vesicles, filipin (500 μg/ml) to inhibit caveolae-mediated uptake, or

Table 1
Physicochemical properties of liposomal l-OHP formulations.

Formulation	Particle size (nm)	Loading efficiency (%)	Zeta potential (mV)
PEG-coated cationic liposome	202.4 ± 14.7	23.6 ± 1.1	+ 11.5 ± 0.9
PEG-coated neutral liposome	200.4 ± 17.2	17.2 ± 3.7	− 7.2 ± 0.5

Data were obtained with three liposome preparations which were prepared independently.

amiloride (10 mM) to inhibit macropinocytosis. Then, DiI-labeled PEG-coated cationic liposomes (4 μmol of lipid/well) were added and the cells were incubated for 1 h at 37 °C in the presence or absence of the inhibitor. The cells were washed once with 1 ml PBS and collected after trypsinisation followed by centrifugation (300 ×g, 4 °C, 5 min). To quench extracellular fluorescence (not internalized liposomes), the cells were treated with 0.3% trypan blue for 5 min at room temperature and resuspended in 0.2 ml of 0.5 mM EDTA-PBS. The cell suspension was analyzed by a flow cytometer as described above.

2.5. Cytotoxicity assay

Cytotoxicity of various l-OHP formulations was determined by MTT assay, as described previously [22]. Briefly, cells (LLCC or HUVEC) were seeded onto 96-well plates at a density of 5×10^2 cells per well 24 h prior to drug addition. The culture medium was replaced with fresh medium (DMEM for LLCC and EBM-2 for HUVEC) containing various concentrations of either free l-OHP, PEG-coated cationic liposomal l-OHP, PEG-coated neutral liposomal l-OHP, or empty PEG-coated cationic liposomes. Following 4 h incubation at 37 °C, the cells were washed twice with PBS and cultured in fresh medium for a further 48 h. After removing the media, 50 μl of MTT stock solution (5 mg/ml in PBS) was added to each well. The cells were further incubated at 37 °C for 4 h. Then, 150 μl of an acidic isopropanol solution (containing 0.04 N HCl) was added to each well to dissolve formazan crystals. The absorbance of each well was read at 570 nm on a microplate reader, Wallac 1420 ARVOsx (PerkinElmer, Trukn, Finland).

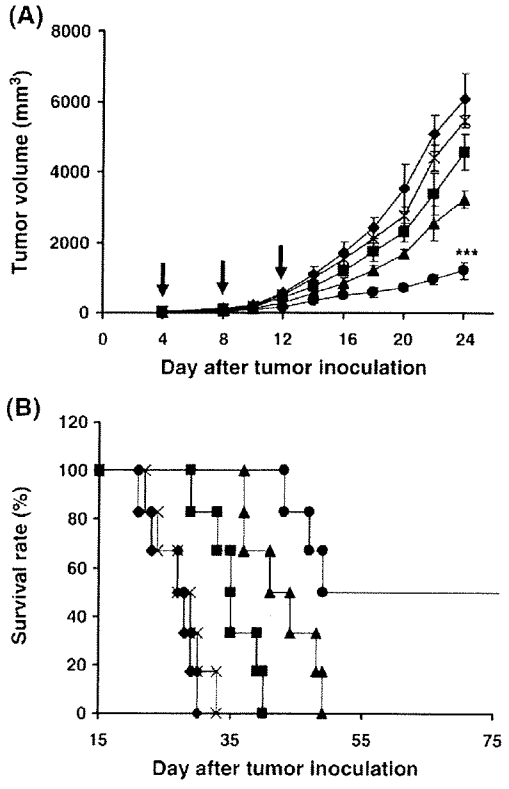

Fig. 1. Antitumor efficacy of various l-OHP formulations on LLCC-tumor bearing mice. On days 4, 8 and 12 after tumor inoculation (indicated by arrows), either free l-OHP (■), l-OHP containing PEG-coated cationic liposomes (●), l-OHP containing PEG-coated neutral liposomes (▲), empty PEG-coated cationic liposomes (x) or 5% dextrose solution (control) (♦) was administered via tail vein at a l-OHP dose of 5 mg/kg. Each treatment group contained 6 mice. (A) Antitumor activity as assessed by tumor size and (B) survival of LLCC-bearing mice. Data in (A) represent mean ± S.D ($n = 6$). ***$p < 0.01$ against other formulations.

Table 2
Summary of median survival time (MST) and percent increased life span (ILS (%)) of tumor-bearing mice after treatment with various l-OHP formulations.

Formulation	MST (days) Median ± SD	ILS (%)
Control (5% dextrose solution)	27.5 ± 3.5	–
Empty PEG-coated cationic liposomes	28.0 ± 4.0	1.8%
Free l-OHP	35.0 ± 3.9	27.3%
PEG-coated neutral l-OHP liposomes	42.0 ± 5.2	52.7%
PEG-coated cationic l-OHP liposomes	>70.0	>150.0%

Data were obtained from Fig. 1B. MST and ILS(%) were calculated with the equations described in the Materials and methods section.

2.6. Evaluation of therapeutic efficacy of l-OHP formulations in the Lewis lung carcinoma bearing mouse model

Male C57BL/6 mice were inoculated subcutaneously (s.c.) at the flank region with LLCC (5×10^5) in a volume of 100 μl (PBS). The mice were divided into five groups. On days 4, 8 and 12 after tumor inoculation, each group (6 mice) received three intravenous injections of either 5% dextrose (control), free l-OHP (5 mg/kg), PEG-coated cationic l-OHP liposomes (5 mg l-OHP/kg), PEG-coated neutral l-OHP liposomes (5 mg l-OHP/kg) or empty PEG-coated cationic liposomes (125 mg total lipid/kg) via tail vain, respectively.

The antitumor activity was evaluated in terms of both tumor volume (mm^3) and survival (%). Tumor dimensions were determined at various time points using a caliper. Tumor volume (mm^3) was calculated using the following formula [23]:

$$\text{Tumor volume}\left(mm^3\right) = \left(a \times b^2\right)/2$$

where a is the length and b is the width in millimeters.

Median survival time (MST (day)) was defined as the time at which half of the mice had died. The percentage increased life span (ILS (%)) was calculated using the following equation [24,25]:

$$\text{ILS (\%)} = [(\text{MST of treated group}/\text{MST of control group}) - 1] \times 100$$

Body weight was measured simultaneously and was taken as a parameter of systemic toxicity.

2.7. In vivo tumor accumulation of DiI-labeled liposomes using in vivo fluorescence imaging

Approximately 5×10^5 of LLCC were inoculated subcutaneously in the flank region of C57BL/6 mice as described above. On day 8 after tumor inoculation (when the tumor volume reached values of 100–120 mm^3), mice were injected with 200 μl of DiI-labeled liposomes (125 mg lipid/kg) via the tail vein. At 6, 24 and 48 h post-injection, mice were anesthetized with isoflurane (FORANE, Abott Japan, Osaka, Japan), a short acting anesthetic, and maintained throughout the imaging process on a heating pad at 37 °C. Fluorescence imaging was performed with Fluorescence Image Analyzer LAS-4000IR (Fujifilm, Tokyo, Japan). The fluorescence images were acquired with a 1/8 s exposure time.

2.8. Determination of l-OHP amount in solid tumor

On day 8 after tumor inoculation, mice were injected intravenously with either l-OHP solution (5 mg/kg) or PEG-coated liposomal l-OHP formulations (5 mg l-OHP/kg, 125 mg total lipid/kg). At 6, 24 or 48 h post-injection, tumors were excised. Tumor tissues were digested according to the following procedure: the tissues were weighed, minced with scissors and placed in glass vials. Then 400 μl of 2 M KOH in isopropanol and 200 μl of H_2O_2 were added, and digestion proceeded by incubation at 65 °C for 12 h. The digested samples

were brought to 1.0 ml with 10% acetic acid and incubated at room temperature for a further 12 h. The content of l-OHP in the sample was then measured by atomic absorption photometry as described previously [10].

2.9. Statistical analysis

All values are expressed as mean ± S.D. Statistical analysis was performed with a two-tailed unpaired t test and one way ANOVA using Graphpad InStat software (GraphPad Software, CA, USA). The level of significance was set at $p<0.05$.

3. Results

3.1. In vivo antitumor activity of l-OHP formulations

The antitumor activity of various l-OHP formulations in Lewis lung carcinoma cell (LLCC) bearing mice was evaluated (Fig. 1). Three sequential administrations with l-OHP formulations showed significant tumor growth suppression (Fig. 1A). The rank order of growth suppression was l-OHP in PEG-coated cationic liposomes >> l-OHP in PEG-coated neutral liposomes > free l-OHP in solution ($p<0.001$, ANOVA). Little tumor growth suppression was observed in mice treated with empty PEG-coated cationic liposomes (no drug). The survival of treated mice are shown in Fig. 1B and the median survival time (MST) and percentage increased life span (ILS (%)) are summarized in Table 2. l-OHP formulations increased the survival of tumor-bearing mice compared with control and empty PEG-coated cationic liposome (no drug). Among the formulations, l-OHP containing PEG-coated cationic liposome showed the strongest effect on the survival of tumor-bearing mice; 50% of the mice (3 out of 6) became long-term survivors (>70 days) ($p<0.001$). In addition, through the therapeutic experiment, no significant body weight loss was observed in any of the treated groups (data not shown). These results suggest that treatment with l-OHP containing PEG-coated cationic liposomes improves the MST of tumor-bearing mice without causing remarkable toxicity.

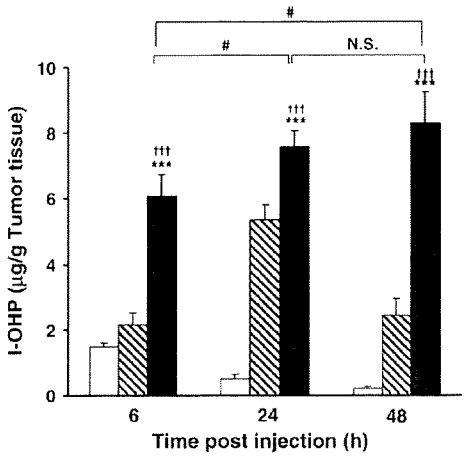

Fig. 3. In vivo tumor accumulation of l-OHP in LLCC-bearing mice. On day 8 after tumor inoculation, mice received an intravenous injection of l-OHP formulation at a dose of 5 mg l-OHP/kg. At 6, 24, or 48 h post injection, tumors were excised. The amount of l-OHP accumulated in tumor tissues was measured as platinum (Pt) using atomic absorption photometry. Open bars, hatched bars and closed bars represent free l-OHP solution, PEG-coated neutral liposomes and PEG-coated cationic liposomes, respectively. Data represent mean ± S.D ($n=3$). $^{\dagger\dagger\dagger}p<0.001$ against free l-OHP, $^{***}p<0.01$ against PEG-coated neutral liposomes, $^{\#}p<0.05$.

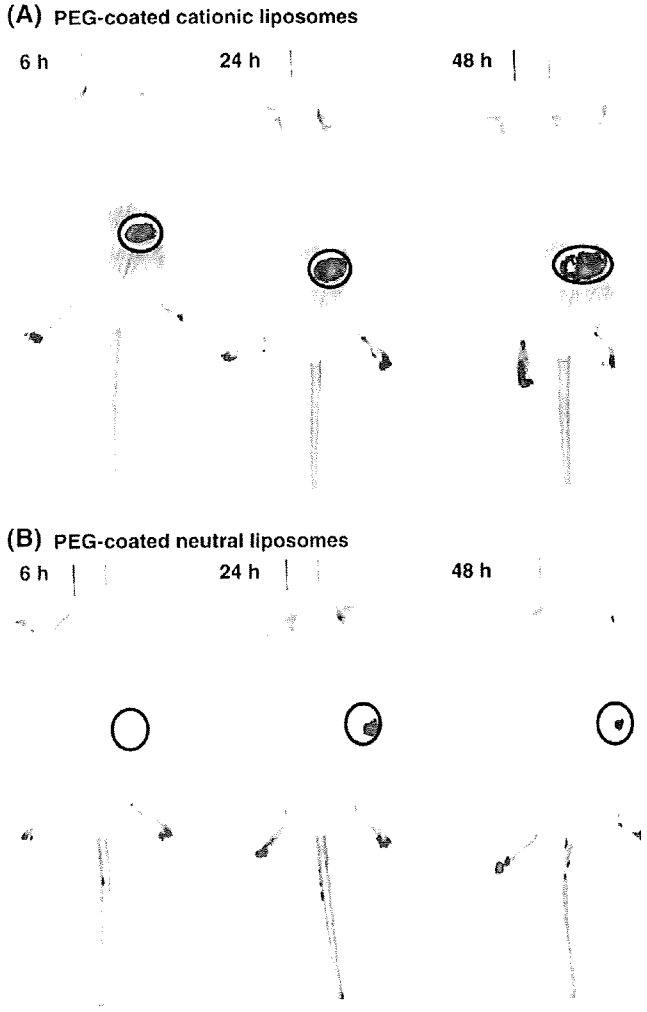

Fig. 2. In vivo tumor accumulation of fluorescently labeled PEG-coated liposomes. On day 8 after tumor inoculation mice received an intravenous injection of fluorescently (DiI) labeled empty PEG-coated liposomes (no drug) at a dose of 125 mg lipid/kg. At 6, 24, and 48 h post injection, in vivo optical images were taken. (A) PEG-coated cationic liposomes. (B) PEG-coated neutral liposomes. All fluorescence images were acquired with a 1/8 s exposure time. Circles indicate tumor locations, not exact tumor areas.

3.2. Accumulation of fluorescently (DiI)-labeled PEG-coated liposomes in solid tumor

Extensive and selective accumulation of drug carriers at the tumor site is essential for the success of in vivo drug targeting to solid tumors. To elucidate whether PEG-coated cationic liposomes accumulate substantially and selectively in a solid tumor than PEG-coated neutral liposomes, fluorescently (DiI)-labeled liposomes were intravenously administered and visualized in the tumor using an in vivo imaging system. Typical representative images are presented in Fig. 2. The fluorescence intensity distribution in the animals is presented in blue color on composite light/fluorescence images. PEG-coated cationic liposomes showed higher levels of accumulation in the tumor than PEG-coated neutral liposomes and accumulation was maintained at such high levels for an extended period (up to 48 h post injection). In addition, the pictures show a much broader area of distribution of PEG-coated cationic liposomes in the tumor region than PEG-coated neutral liposomes. These findings suggest that the PEG-coated cationic liposomes we recently developed [10], is a promising carrier for the achievement of tumor-targeted drug delivery.

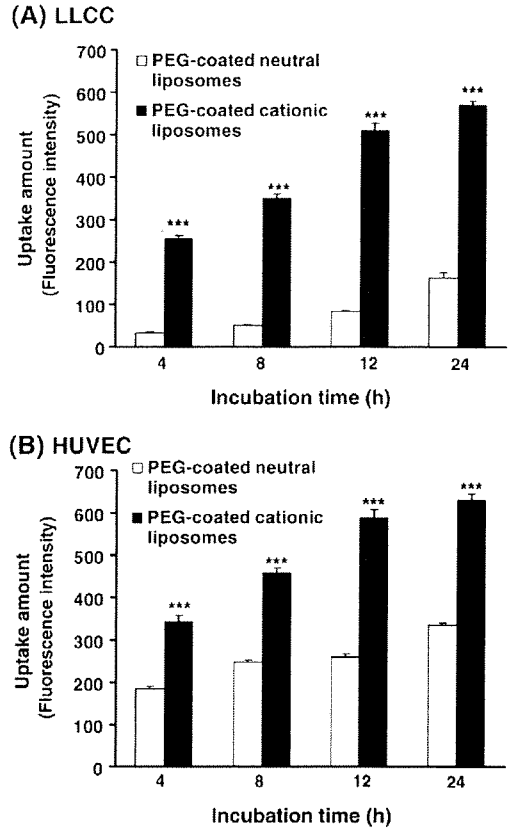

Fig. 4. Uptake of fluorescently labeled PEG-coated liposomes by LLCC and HUVEC. Cells (LLCC or HUVEC) were incubated with either DiI-labeled empty PEG-coated cationic liposomes or PEG-coated neutral liposomes. At 4, 8, 12 and 24 h post incubation, the cells were collected and the fluorescence of non internalized liposomes was quenched by incubating with 0.3% trypan blue solution. Then the cells were analyzed by flow cytometry. (A) LLCC. (B) HUVEC. Data represent the mean of three independent experiments ± S.D. ***$p < 0.001$ against PEG-coated neutral liposomes.

3.3. Accumulation of l-OHP in solid tumor

Mice bearing a LLCC solid tumor were treated with intravenous injection of either free l-OHP or liposomal l-OHP formulations to examine intra-tumoral l-OHP disposition (Fig. 3). Maximum intra-tumor accumulation of free l-OHP occurred at 6 h post-injection and gradually decreased to near zero levels by 48 h after injection. With PEG-coated neutral liposomes a 3-fold higher maximal l-OHP accumulation was achieved than with free l-OHP, but this value was reached only after 24 h, but at 48 h the level was still higher than the maximal level obtained with free 1-OHP. On the other hand, with PEG-coated cationic liposomes a 3-fold higher level of l-OHP was obtained after 6 h than with PEG-coated neutral liposomes while accumulation still increased up to 24 h and was sustained for at least another 24 h till 48 h post-injection.

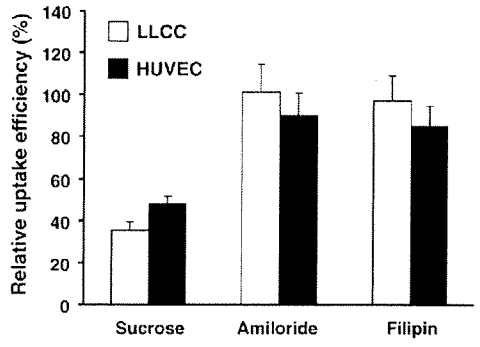

Fig. 5. Effects of inhibitors on cellular uptake of PEG-coated cationic liposomes. Cells (LLCC or HUVEC) were pre-incubated with various inhibitors for 30 min at 37 °C. Then fluorescently (DiI) labeled PEG-coated cationic liposomes (no drug) (4 μmol lipids/well) were added and the cells were further incubated for 1 h. After incubation the cells were collected and analyzed by flow cytometry following treatment with 0.3% trypan blue solution to quench fluorescence of extracellularly adhering non-internalized liposomes. Fluorescence intensity of DiI in untreated cells, representing the maximum internalized amount of PEG-coated cationic liposomes, was taken as 100%. Data represent mean ± S.D. ($n = 3$).

Table 3
In vitro cytotoxicity of various l-OHP formulations.

Formulation	IC_{50} (μM)	
	LLCC	HUVEC
Free l-OHP	7.9 ± 0.1	16.0 ± 1.0
PEG-coated cationic l-OHP liposomes	34.7 ± 0.9***	85.4 ± 5.7***
PEG-coated neutral l-OHP liposomes	115.4 ± 0.7***, †††	218.8 ± 8.0***, †††

Cells were incubated with media containing serial dilutions of various l-OHP formulations (free l-OHP, l-OHP containing PEG-coated cationic liposomes and l-OHP containing PEG-coated neutral liposomes). Following a 4-h incubation at 37 °C, the medium was replaced with fresh medium and incubated for a further 48 h. Then cell survival was determined by the MTT assay. Data represent mean ± S.D. ($n = 3$) ***$p < 0.001$ against free l-OHP, †††$p < 0.001$ against PEG-coated l-OHP neutral liposomes.

3.4. In vitro cellular uptake of fluorescently (DiI)-labeled PEG-coated liposomes

Fig. 4 shows that much larger amounts of PEG-coated cationic liposomes are internalized by both cell lines (LLCC and HUVEC) than of PEG-coated neutral liposomes. For both liposome formulations the amounts taken up gradually increased with time up to 24 h. In order to elucidate the uptake mechanism of the PEG-coated cationic liposomes, the effect of various endocytosis inhibitors on the uptake efficiency was investigated. Among the three inhibitors used (hypertonic sucrose, filipin and amiloride), only hypertonic sucrose extensively inhibited cellular uptake of PEG-coated cationic liposomes in both LLCC and HUVEC (Fig. 5). This indicates that the PEG-coated cationic liposomes are internalized by LLCC and HUVEC mainly via a clathrin-mediated endocytosis pathway.

3.5. Cytotoxicity of l-OHP formulations

The cytotoxicity of l-OHP formulations and empty PEG-coated cationic liposomes was investigated. As summarized in Table 3, for both LLCC and HUVEC, the IC_{50} value of l-OHP encapsulated in PEG-coated cationic liposome was much lower than that of l-OHP encapsulated in PEG-coated neutral liposome ($p < 0.001$). Both liposomal l-OHP formulations were significantly less cytotoxic in both cell lines than free l-OHP ($p < 0.001$). It appears that LLCC are more sensitive to l-OHP than HUVEC. In addition, empty PEG-coated cationic liposomes did not show any cytotoxicity at lipid concentrations corresponding to the l-OHP containing PEG-coated cationic liposomes we tested (not shown).

4. Discussion

We recently developed a PEG-coated cationic liposome and confirmed that such cationic liposome is a promising carrier delivering encapsulated chemotherapeutic agents to the tumor endothelium [10]. In addition, we showed that l-OHP containing PEG-coated cationic liposomes can bring about a potent anti-angiogenic effect in a mouse dorsal air sac (DAS) model [10]. Following up on these results, in the present study we aimed at investigating the antitumor effect of the l-OHP formulation in a murine tumor-xenograft model and providing an insight into the

probable mechanism of the enhanced antitumor effect of such l-OHP formulation.

An in vivo imaging study demonstrated a rapid accumulation and a more extensive intra-tumoral distribution of PEG-coated cationic liposomes in the solid tumor than of PEG-coated neutral liposomes (Fig. 2). Both PEG-coated liposomes, once administered in the blood stream, are expected to easily and efficiently gain access to the tumor tissue because of their prolonged circulation time in the blood compartment [14–16,26,27]. However, only PEG-coated cationic liposomes are able to selectively bind to endothelial cells in the tumor vasculature due to electrostatic interaction between the cationic surface charge of the liposome and negative charge of the plasma membrane of the endothelial cells as demonstrated earlier [10]. This notion was supported by our in vitro binding study using HUVEC, demonstrating that PEG-coated cationic liposomes massively associate with and are internalized by this endothelial cell line, regardless of the presence of PEG coating (Fig. 4B). Thurston et al. [11] also showed that cationic liposomes accumulate selectively in the vasculature of tumors, in contrast to anionic, neutral or PEG-coated neutral liposomes.

The in vivo imaging study also showed that the PEG-coated cationic liposomes are retained in the tumor tissue for a longer period than PEG-coated neutral liposomes (Fig. 2A). The continuous supply of PEG-coated cationic liposomes to the tumor tissue might saturate their binding sites on tumor vascular endothelial cells and thus facilitate their extravasation into the tumor interstitial space due to the EPR effect [17]. Upon diffusion into the interstitial space, the PEG-coated cationic liposomes are likely to bind to and subsequently to be internalized by the tumor cells as a result of electric interactions as shown in Figs. 4A and 5. This will result in prolonged retention time of the liposome in the tumor tissue (Fig. 2). Similar observations have been reported for PEG-coated liposomes modified with transferrin (Tf) [8,28,29]. On the other hand, PEG-coated neutral liposomes although also efficiently accumulating in the tumor tissue, albeit less rapidly than the cationic liposomes, are gradually eliminated from the tissue (Fig. 2). This is most likely explained by the lack of anchor (electric force) of the liposome preventing it from engaging in electrostatic interactions with endothelial cells and/or tumor cells (Fig. 4).

Quantitative determination of l-OHP in the tumor (Fig. 3) demonstrated that encapsulation in PEG-coated cationic liposomes causes l-OHP to rapidly accumulate and be retained in the tumor tissue, while PEG-coated neutral liposome resulted in slow l-OHP accumulation in and rapid elimination from the tissue. The accumulation patterns of l-OHP were very similar to those of the liposomes themselves, as visualized by the in vivo imaging system (Fig. 2). In addition, we recently reported that both liposomal l-OHP formulations retained 60–65% of encapsulated l-OHP in the presence of 50% mouse plasma following a 24-h incubation at 37 °C [10]. Accordingly, it was concluded, in terms of therapeutic efficacy, that PEG-coated cationic liposomes provide a superior efficiency in delivering l-OHP inside tumor tissue, thereby resulting in efficient tumor growth suppression and increased survival time of tumor bearing mice (Fig. 1 and Table 2). Generally, to obtain increased therapeutic efficacy, a drug carrier must achieve not only increased delivery of the drug in the tumor tissue but also enhanced interaction of the drug with and subsequent internalization by tumor cells. Although the exact mechanism by which the increased therapeutic efficacy in this study was obtained still is not clear, the results from our in vitro studies (Figs. 4 and 5 and Table 3) support the notion that, once accumulated in the tumor tissue, the PEG-coated cationic liposomes were presumably internalized by endothelial cells as well as tumor cells, and consequently delivered the encapsulated l-OHP in the cytoplasm of those cells. l-OHP, once delivered in the cytoplasm, would be retained for a long time (Fig. 3) due to the irreversible formation of complexes with proteins, DNA and other cellular macromolecules [30].

In contrast to cisplatin, l-OHP has no renal toxicity, only mild hematological and gastrointestinal toxicity, while neurotoxicity is dose-limiting [4,5]. The selective delivery of l-OHP to tumor tissues by the PEG-coated cationic liposome raises the possibility of reducing such toxicity. Actually, in this study, l-OHP containing PEG-coated cationic liposome did not show any remarkable side effect. Many studies have documented the specialization of the vasculature in tumors, both with respect to structural abnormalities and to potential molecular targets [31,32]. Cationic liposomes have been shown to associate readily with the endothelium of tumor vessels [11,33–38]. A recent study indicated that PEG-coated cationic liposomes associate with approximately 27 and 5% of vessel areas in tumors and normal tissues, respectively, in human and murine tumor models [39]. In our earlier study, we also observed a lack of selective accumulation/binding of the PEG-coated cationic liposomes to pre-existing blood vessels in the skin of the DAS model [10]. This points to an important difference in distribution of the liposomes between the vasculature of tumor tissue and that of normal tissues, which may be exploited while attempting to reduce the toxicity of l-OHP. Nevertheless, the cumulative toxicity of cationic liposomal anticancer drug formulations following several sequential administrations has not been evaluated yet. Further systemic experiments following long-term treatments with our l-OHP formulation are currently underway in our laboratory.

Recent efforts have focused on the application of various combination treatment regimens that include cytotoxic and anti-angiogenic agents, to improve the overall antitumor response in preclinical models in vivo [40]. However, preclinical and clinical studies have indicated that the toxicity profile of such combinations differs from that of conventional single chemotherapy, thus ruling out additive toxicity as a major limitation of the combination chemotherapy [41,42]. In this study, we demonstrated that l-OHP containing PEG-coated cationic liposomes exert their efficient antitumor activity probably via a dual targeting approach, addressing not only the tumor endothelium but also the tumor cells. A dual mechanism of action has been proposed by Pastorino et al. [18,19]: indirect tumor cell kill via the destruction of tumor endothelium by doxorubicin (DXR)-containing liposomes targeted to aminopeptidase N (NGR-targeted DXR liposomes) and direct tumor cell kill via delivery of liposomal DXR to the tumor interstitial space. Such dual targeting approach, vascular-targeting and tumor-targeting with a single liposomal anticancer drug formulation, may have strong potential to overcome some major limitations in conventional anticancer chemotherapy.

5. Conclusion

In this study, we showed that with l-OHP containing PEG-coated cationic liposomes a remarkable tumor growth suppression and increased survival time of tumor-bearing mice can be achieved, without apparent side effects, presumably as a result of delivering the encapsulated drug to both blood vessels located specifically at tumor sites and to the tumor cells themselves. The dual targeting approach, vascular-targeting and tumor-targeting with a single liposomal anticancer drug formulation, may have the potential to overcome some of the major shortcomings of conventional chemotherapeutic strategies.

Acknowledgments

We thank Dr. G.L. Scherphof for his helpful advice in preparing this manuscript. This study was supported, in part, by the Kobayashi Fund for Cancer Research and the Knowledge Cluster Initiative from Ministry of Education, Science and Technology.

References

[1] A. Ibrahim, S. Hirschfeld, M.H. Cohen, D.J. Griebel, G.A. Williams, R. Pazdur, FDA drug approval summaries: oxaliplatin, Oncologist 9 (2004) 8–12.
[2] C. Tournigand, T. Andre, E. Achille, G. Lledo, M. Flesh, D. Mery-Mignard, E. Quinaux, C. Couteau, M. Buyse, G. Ganem, B. Landi, P. Colin, C. Louvet, A. de Gramont, FOLFIRI

followed by FOLFOX6 or the reverse sequence in advanced colorectal cancer: a randomized GERCOR study, J. Clin. Oncol. 22 (2004) 229–237.
[3] A. Pessino, A. Sobrero, Optimal treatment of metastatic colorectal cancer, Expert Rev. Anticancer Ther. 6 (2006) 801–812.
[4] A. Grothey, Oxaliplatin-safety profile: neurotoxicity, Semin. Oncol. 30 (2003) 5–13.
[5] A. Pietrangeli, M. Leandri, E. Terzoli, B. Jandolo, C. Garufi, Persistence of high-dose oxaliplatin-induced neuropathy at long-term follow-up, Eur. Neurol. 56 (2006) 13–16.
[6] L. Pendyala, P.J. Creaven, In vitro cytotoxicity, protein binding, red blood cell partitioning, and biotransformation of oxaliplatin, Cancer Res. 53 (1993) 5970–5976.
[7] H. Cabral, N. Nishiyama, K. Kataoka, Optimization of (1,2-diamino-cyclohexane) platinum(II)-loaded polymeric micelles directed to improved tumor targeting and enhanced antitumor activity, J. Control. Release 121 (2007) 146–155.
[8] R. Suzuki, T. Takizawa, Y. Kuwata, M. Mutoh, N. Ishiguro, N. Utoguchi, A. Shinohara, M. Eriguchi, H. Yanagie, K. Maruyama, Effective anti-tumor activity of oxaliplatin encapsulated in transferrin-PEG-liposome, Int. J. Pharm. 346 (2008) 143–150.
[9] G.P. Stathopoulos, T. Boulikas, A. Kourvetaris, J. Stathopoulos, Liposomal oxaliplatin in the treatment of advanced cancer: a phase I study, Anticancer Res. 26 (2006) 1489–1493.
[10] A. Abu-Lila, T. Suzuki, Y. Doi, T. Ishida, H. Kiwada, Oxalipalatin targeting to angiogenic vessels by PEGylated cationic liposomes suppresses the angiogenesis in a dosal air sac model, J. Control. Release 134 (2009) 18–25.
[11] G. Thurston, J.W. McLean, M. Rizen, P. Baluk, A. Haskell, T.J. Murphy, D. Hanahan, D.M. McDonald, Cationic liposomes target angiogenic endothelial cells in tumors and chronic inflammation in mice, J. Clin. Invest. 101 (1998) 1401–1413.
[12] T. Nomura, N. Koreeda, F. Yamashita, Y. Takakura, M. Hashida, Effect of particle size and charge on the disposition of lipid carriers after intratumoral injection into tissue-isolated tumors, Pharm. Res. 15 (1998) 128–132.
[13] J. Wu, A. Lee, Y. Lu, R.J. Lee, Vascular targeting of doxorubicin using cationic liposomes, Int. J. Pharm. 337 (2007) 329–335.
[14] T.M. Allen, C. Hansen, F. Martin, C. Redemann, A. Yau-Young, Liposomes containing synthetic lipid derivatives of poly(ethylene glycol) show prolonged circulation half-lives in vivo, Biochim. Biophys. Acta 1066 (1991) 29–36.
[15] C. Allen, N. Dos Santos, R. Gallagher, G.N. Chiu, Y. Shu, W.M. Li, S.A. Johnstone, A.S. Janoff, L.D. Mayer, M.S. Webb, M.B. Bally, Controlling the physical behavior and biological performance of liposome formulations through use of surface grafted poly(ethylene glycol), Biosci. Rep. 22 (2002) 225–250.
[16] A.L. Klibanov, K. Maruyama, A.M. Beckerleg, V.P. Torchilin, L. Huang, Activity of amphipathic poly(ethylene glycol) 5000 to prolong the circulation time of liposomes depends on the liposome size and is unfavorable for immunoliposome binding to target, Biochim. Biophys. Acta 1062 (1991) 142–148.
[17] Y. Matsumura, H. Maeda, A new concept for macromolecular therapeutics in cancer chemotherapy: mechanism of tumoritropic accumulation of proteins and the antitumor agent smancs, Cancer Res. 46 (1986) 6387–6392.
[18] F. Pastorino, C. Brignole, D. Marimpietri, M. Cilli, C. Gambini, D. Ribatti, R. Longhi, T.M. Allen, A. Corti, M. Ponzoni, Vascular damage and anti-angiogenic effects of tumor vessel-targeted liposomal chemotherapy, Cancer Res. 63 (2003) 7400–7409.
[19] F. Pastorino, C. Brignole, D. Di Paolo, B. Nico, A. Pezzolo, D. Marimpietri, G. Pagnan, F. Piccardi, M. Cilli, R. Longhi, D. Ribatti, A. Corti, T.M. Allen, M. Ponzoni, Targeting liposomal chemotherapy via both tumor cell-specific and tumor vasculature-specific ligands potentiates therapeutic efficacy, Cancer Res. 66 (2006) 10073–10082.
[20] G.R. Bartlett, Colorimetric assay methods for free and phosphorylated glyceric acids, J. Biol. Chem. 234 (1959) 469–471.
[21] T.C. Stover, Y.S. Kim, T.L. Lowe, M. Kester, Thermoresponsive and biodegradable linear-dendritic nanoparticles for targeted and sustained release of a pro-apoptotic drug, Biomaterials 29 (2008) 359–369.
[22] K. Atobe, T. Ishida, E. Ishida, K. Hashimoto, H. Kobayashi, J. Yasuda, T. Aoki, K. Obata, H. Kikuchi, H. Akita, T. Asai, H. Harashima, N. Oku, H. Kiwada, In vitro efficacy of a sterically stabilized immunoliposomes targeted to membrane type 1 matrix metalloproteinase (MT1-MMP), Biol. Pharm. Bull. 30 (2007) 972–978.
[23] J.H. Kim, Y.S. Kim, K. Park, S. Lee, H.Y. Nam, K.H. Min, H.G. Jo, J.H. Park, K. Choi, S.Y. Jeong, R.W. Park, I.S. Kim, K. Kim, I.C. Kwon, Antitumor efficacy of cisplatin-loaded glycol chitosan nanoparticles in tumor-bearing mice, J. Control. Release 127 (2008) 41–49.
[24] M.R. Kviecinski, K.B. Felipe, T. Schoenfelder, L.P. de Lemos Wiese, M.H. Rossi, E. Goncalez, J.D. Felicio, D.W. Filho, R.C. Pedrosa, Study of the antitumor potential of *Bidens pilosa* (Asteraceae) used in Brazilian folk medicine, J. Ethnopharmacol. 117 (2008) 69–75.
[25] D.E. Lopes de Menezes, L.M. Pilarski, A.R. Belch, T.M. Allen, Selective targeting of immunoliposomal doxorubicin against human multiple myeloma in vitro and ex vivo, Biochim. Biophys. Acta 1466 (2000) 205–220.
[26] K. Kawahara, A. Sekiguchi, E. Kiyoki, T. Ueda, K. Shimamura, Y. Kurosaki, S. Miyaoka, H. Okabe, M. Miyajima, J. Kimura, Effect of TRX-liposomes size on their prolonged circulation in rats, Chem. Pharm. Bull. (Tokyo) 51 (2003) 336–338.
[27] K. Morimoto, M. Kondo, K. Kawahara, H. Ushijima, Y. Tomino, M. Miyajima, J. Kimura, Advances in targeting drug delivery to glomerular mesangial cells by long circulating cationic liposomes for the treatment of glomerulonephritis, Pharm. Res. 24 (2007) 946–954.
[28] O. Ishida, K. Maruyama, H. Tanahashi, M. Iwatsuru, K. Sasaki, M. Eriguchi, H. Yanagie, Liposomes bearing polyethyleneglycol-coupled transferrin with intracellular targeting property to the solid tumors in vivo, Pharm. Res. 18 (2001) 1042–1048.
[29] S. Sofou, G. Sgouros, Antibody-targeted liposomes in cancer therapy and imaging, Expert Opin. Drug Deliv. 5 (2008) 189–204.
[30] M.A. Graham, G.F. Lockwood, D. Greenslade, S. Brienza, M. Bayssas, E. Gamelin, Clinical pharmacokinetics of oxaliplatin: a critical review, Clin. Cancer Res. 6 (2000) 1205–1218.
[31] D. Fukumura, R.K. Jain, Tumor microvasculature and microenvironment: targets for anti-angiogenesis and normalization, Microvasc. Res. 74 (2007) 72–84.
[32] D. Fukumura, R.K. Jain, Tumor microenvironment abnormalities: causes, consequences, and strategies to normalize, J. Cell. Biochem. 101 (2007) 937–949.
[33] R.B. Campbell, D. Fukumura, E.B. Brown, L.M. Mazzola, Y. Izumi, R.K. Jain, V.P. Torchilin, L.L. Munn, Cationic charge determines the distribution of liposomes between the vascular and extravascular compartments of tumors, Cancer Res. 62 (2002) 6831–6836.
[34] R.B. Campbell, B. Ying, G.M. Kuesters, R. Hemphill, Fighting cancer: from the bench to bedside using second generation cationic liposomal therapeutics, J. Pharm. Sci. 98 (2009) 411–429.
[35] S. Strieth, M.E. Eichhorn, A. Werner, B. Sauer, M. Teifel, U. Michaelis, A. Berghaus, M. Dellian, Paclitaxel encapsulated in cationic liposomes increases tumor microvessel leakiness and improves therapeutic efficacy in combination with cisplatin, Clin. Cancer Res. 14 (2008) 4603–4611.
[36] S. Strieth, C.F. Nussbaum, M.E. Eichhorn, M. Fuhrmann, M. Teifel, U. Michaelis, A. Berghaus, M. Dellian, Tumor-selective vessel occlusions by platelets after vascular targeting chemotherapy using paclitaxel encapsulated in cationic liposomes, Int. J. Cancer 122 (2008) 452–460.
[37] C.R. Dass, P.F. Choong, Selective gene delivery for cancer therapy using cationic liposomes: in vivo proof of applicability, J. Control. Release 113 (2006) 155–163.
[38] C.R. Dass, P.F. Choong, Targeting of small molecule anticancer drugs to the tumour and its vasculature using cationic liposomes: lessons from gene therapy, Cancer Cell Int. 6 (2006) 17.
[39] A.V. Kalra, R.B. Campbell, Development of 5-FU and doxorubicin-loaded cationic liposomes against human pancreatic cancer: implications for tumor vascular targeting, Pharm. Res. 23 (2006) 2809–2817.
[40] S. Ghosh, P. Maity, Augmented antitumor effects of combination therapy with VEGF antibody and cisplatin on murine B16F10 melanoma cells, Int. Immunopharmacol. 7 (2007) 1598–1608.
[41] M. Martinelli, K. Bonezzi, E. Riccardi, E. Kuhn, R. Frapolli, M. Zucchetti, A.J. Ryan, G. Taraboletti, R. Giavazzi, Sequence dependent antitumour efficacy of the vascular disrupting agent ZD6126 in combination with paclitaxel, Br. J. Cancer 97 (2007) 888–894.
[42] J.J. Knox, D. Hedley, A. Oza, R. Feld, L.L. Siu, E. Chen, M. Nematollahi, G.R. Pond, J. Zhang, M.J. Moore, Combining gemcitabine and capecitabine in patients with advanced biliary cancer: a phase II trial, J. Clin. Oncol. 23 (2005) 2332–2338.

Journal of Controlled Release 134 (2009) 194–200

Contents lists available at ScienceDirect

Journal of Controlled Release

journal homepage: www.elsevier.com/locate/jconrel

Synergistic antitumor activity of metronomic dosing of cyclophosphamide in combination with doxorubicin-containing PEGylated liposomes in a murine solid tumor model

Tatsuhiro Ishida *, Emi Shiraga, Hiroshi Kiwada

Department of Pharmacokinetics and Biopharmaceutics, Subdivision of Biopharmaceutical Science, Institute of Health Biosciences, The University of Tokushima, 1-78-1, Sho-machi, Tokushima 770-8505, Japan

ARTICLE INFO

Article history:
Received 5 September 2008
Accepted 18 November 2008
Available online 3 December 2008

Keywords:
Combination therapy
Metronomic chemotherapy
Liposomal anticancer drug
PEGylated liposome
Cyclophosphamide
Doxorubicin

ABSTRACT

Cyclophosphamide (CPA) and doxorubicin (DXR)-containing sterically stabilized liposomes (DXR-SL) have a proven clinical activity. We propose that a metronomic CPA dosing schedule enhances accumulation of DXR-SL in solid tumors, because it causes apoptosis in the endothelial cells of the growing tumor vasculature and thereby may increase the permeability of the tumor microvessels. To establish the validity of this hypothesis we investigated the therapeutic benefits of metronomic CPA dosing (p.o.) combined with DXR-SL (i.v.) in a Lewis lung carcinoma, subcutaneously growing in C57BL/6 mouse. The metronomic CPA dosing clearly promoted accumulation and subsequent deep diffusion of SL in the solid tumor as a result of rather a transient increase in the density of $CD31^+$-microvessels, which shows high permeability to SL. It appears that the enhancing effect of metronomic CPA dosing is strongly dependent on the dose of CPA as well as on the time at which the treatment was initiated. Our study indicates that the use of metronomic chemotherapy combined with nanocarriers may be of significant clinical and practical importance in treating intractable solid tumors.

© 2008 Elsevier B.V. All rights reserved.

1. Introduction

In conventional chemotherapy with anticancer agents, the therapeutic agent is usually administered in short courses of therapy using the maximum tolerated dose (MTD chemotherapy). MTD chemotherapy requires prolonged drug-free breaks between successive cycles of therapy due to toxicity [1]. As an elegant alternative approach, a novel chemotherapeutic regimen, metronomic chemotherapy, has been advocated in recent years [1–3] implying the frequent administration of an anticancer agent at doses significantly below the MTD. This approach, which clearly shows lower toxicity, without the need for prolonged drug-free breaks, may also have potential for antitumor strategies involving a secondary alternative mechanism, i.e. inhibition of tumor angiogenesis [1–3]. Among various anticancer agents, cyclophosphamide (CPA), a traditional alkylating agent, is most frequently used for metronomic chemotherapy [4,5]. At lower doses, CPA is thought to induce apoptosis in tumor endothelial cells, subsequent collapse of angiogenic vessels, and ultimately suppression of tumor growth [6].

Liposomes were one of the first nanoparticulate drug delivery systems to show increased delivery of low molecular weight anticancer agents to solid tumors. Liposomes with diameters in the range of 100 nm can accumulate in solid tumors via the enhanced permeability and retention (EPR) effect [7], which occurs when nanoparticulates extravasate from the circulation into tumors through gaps in the vasculature endothelium [8]. The ability of liposomes to localize in solid tumors via the EPR effect partly depends on their long circulating properties, which can be achieved by grafting polyethylene glycol (PEG) to the surface of the liposomes (sterically stabilized liposomes (SL)) [9]. Anticancer agents encapsulated in SL have shown increased efficiency and lower toxicity in treatment of solid tumors by achieving higher accumulation in tumor tissue but limited accumulation in healthy organs [10,11]. Doxorubicin-containing SL (DXR-SL), Doxil/Caelyx, has been approved for clinical use [12,13].

Given the apoptosis induction potency of CPA in endothelial cells of growing tumor vasculature [6], we propose that a metronomic CPA-dosing schedule will increase the permeability of tumor microvessels to DXR-SL, resulting in a further enhanced accumulation of DXR in solid tumors. This may raise the possibility of increasing the therapeutic efficacy of liposomal DXR as well as a reduction in the total DXR dose. The reduction of DXR dose may improve tolerance of

Abbreviations: Ab, antibody; CHOL, cholesterol; CPA, cyclophosphamide; DiI, 1, 1′-dioctadecyl-3, 3, 3′, 3′-tetramethylindocarbocyanine perchlorate; DXR, doxorubicin; DXR-SL, DXR-containing sterically stabilized liposome; EPR, enhanced permeability and retention; FBS, fetal bovine serum; FITC, fluorescein isothiocyanate; HEPC, hydrogenated egg phosphatidylcholine; $mPEG_{2000}$-DSPE, 1, 2-distearoyl-*sn*-glycero-3-phosphoethanolamine-*n*-[methoxy(polyethylene glycol)-2000]; MTD, maximum tolerated dose; PEG, polyethylene glycol; SL, sterically stabilized liposome.

* Corresponding author. Tel./fax: +81 88 633 7260.
E-mail address: ishida@ph.tokushima-u.ac.jp (T. Ishida).

0168-3659/$ – see front matter © 2008 Elsevier B.V. All rights reserved.
doi:10.1016/j.jconrel.2008.11.019

patients and thereby improve therapeutic efficacy as compared to the conventional DXR therapy. In this study we therefore determined the efficacy of the combination of two anticancer agents, i.e. CPA and DXR-SL, using Lewis lung carcinoma, subcutaneously growing in C57BL/6 mice, as a model. In addition, we examined if metronomic CPA dosing truly enhances accumulation of SL in solid tumors as a result of an interference with the formation of the tumor vasculature.

2. Materials and methods

2.1. Materials

Hydrogenated egg phosphatidylcholine (HEPC) and 1, 2-distearoyl-*sn*-glycero-3-phosphoethanolamine-*n*-[methoxy(polyethylene glycol)-2000] ($mPEG_{2000}$-DSPE) were generously donated by NOF (Tokyo, Japan). Doxorubicin (DXR), cholesterol (CHOL) and cyclophosphamide (CPA) were purchased from Wako Pure Chemical (Osaka, Japan). FITC (fluorescein isothiocyanate)-labeled rabbit anti-rat IgG heavy and light chain polyclonal antibody (Ab) was purchased from Abcam (Cambridge, UK). Rat monoclonal anti-mouse CD45 Ab was purchased from R&D systems (CA, USA). FITC-labeled rat monoclonal anti-mouse CD31 Ab was purchased from Millipore (MA, USA). DiI (1, 1′-dioctadecyl-3, 3, 3′, 3′-tetramethylindocarbocyanine perchlorate) was purchased from Invitrogen (Paisley, UK). All other reagents were of analytical grade.

2.2. Animals and tumor cell line

Male C57BL/6 mice, 5 weeks old, were purchased from Japan SLC (Shizuoka, Japan). The experimental animals were allowed free access to water and mouse chow, and were housed under controlled environmental conditions (constant temperature, humidity, and a 12-h dark–light cycle). All animal experiments were evaluated and approved by the Animal and Ethics Review Committee of the University of Tokushima.

Lewis lung carcinoma cells were maintained in DMEM (Wako Pure Chemical) supplemented with 10% heat-inactivated fetal bovine serum (FBS) (Japan Bioserum, Hiroshima, Japan), 10 mM L-glutamine, 100 U/mL penicillin and 100 μg/mL streptomycin in a 5% CO_2/air atmosphere at 37 °C.

2.3. Preparation of liposomes

SL was composed of HEPC/CHOL/$mPEG_{2000}$-DSPE (2/1/0.1 molar ratio). Liposomes were prepared using the thin-film hydration technique, as previously described [14,15]. DiI labeled liposomes were prepared by the addition of DiI to the lipid mixture (1% related to total lipid) before formulation of a thin-film layer. The mean diameter of the liposomes was approximately 100 nm, as determined using a NICOMP 370 HPL submicron particle analyzer (Particle Sizing System, CA, USA). The phospholipid concentration was determined by a colorimetric assay [16]. DXR was encapsulated into the liposomes by remote loading using an ammonium sulfate gradient, as previously described [17]. After loading DXR into the liposomes, unencapsulated DXR was removed using a Sephadex G-50 column in 25 mM HEPES buffered saline (pH 7.4). DXR-loading efficiency was >90%.

2.4. Tumor model and assessment of antitumor effect

Lewis lung carcinoma cells were grown to 80–90% confluence in a 10 cm culture dish, harvested by treatment with trypsin, and resuspended in DMEM containing 10% FBS. The cells (5×10^5) in 0.1 mL DMEM were injected subcutaneously into the left flank of C57BL/6 mice. Most tumors reached a volume of approximately 50 mm^3 at day 5 and 1000 mm^3 at day 12, respectively. Treatments described below were started at day 5 or day 12 after inoculating the tumor cells.

Xenograft tumors were measured externally every third day. A group in which the treatment was started at day 5 was monitored from day 5 until day 29. The other group, in which is treatment was started at day 12, was monitored from day 6 until day 30. Tumor volume was approximated by using the equation $vol=(a\times b^2)/2$, where vol is volume, a the length of the major axis, and b is the length of the minor axis. The index of tumor-growth suppression was calculated as follows: The group in which the treatments were started at day 5 was calculated with the formula; [{1−(tumor growth of treated group on day 24)/(tumor growth of control on day 24)}×100]. The group in which the treatments were started at day 12 was calculated with the formula; [{1−(tumor growth of treated group on day 27)/(tumor growth of control on day 27)}×100].

2.5. CPA and DXR-SL dosing schedules

Treatments described below were started at either day 5 or day 12 after inoculating the tumor cells as follows:

(1) *Conventional CPA-dosing.* Mice ($n=5$) received a total 3 doses of CPA (150 mg/kg per dose) administered subcutaneously every other day (total dose: 450 mg/kg, i.e., MTD) [6,15].
(2) *Metronomic CPA-dosing. Group A*; mice ($n=5$) received eight doses of CPA (20 or 60 mg/kg per dose) administered orally at 3-day intervals (total dose: 160 or 480 mg/kg). The treatment was started at day 5 after tumor-inoculation. *Group B*; mice ($n=5$) received six doses of CPA (20 or 60 mg/kg per dose) administered orally at 3-day intervals (total dose: 120 or 360 mg/kg). The treatment was started at day 12 after tumor-inoculation.
(3) *Conventional DXR-SL dosing. Group A*; mice ($n=5$) received eight doses of DXR-SL (1 mg/kg) intravenously at 3-day intervals (total dose: 8 mg/kg). The treatment was started at day 5 after tumor-inoculation. *Group B*; mice ($n=5$) received six doses of DXR-SL (1 mg/kg) intravenously at 3-day intervals (total dose: 6 mg/kg). The treatment was started at day 12 after tumor-inoculation.
(4) *Combination of CPA dosing with DXR-SL dosing. Group A*; mice ($n=5$) received eight doses of CPA (20 or 60 mg/kg per dose, total dose: 160 or 480 mg/kg) administered orally and eight doses of DXR-SL (1 mg/kg per dose, total dose: 8 mg/kg) administered intravenously at 3-day intervals. The treatment was started at day 5 after tumor-inoculation. *Group B*; mice ($n=5$) received six doses of CPA (20 or 60 mg/kg per dose, total dose: 120 or 360 mg/kg) administered orally and six doses of DXR-SL (1 mg/kg per dose, total dose: 6 mg/kg) administered intravenously at 3-day intervals. The treatment was started at day 12 after tumor-inoculation.

2.6. $CD31^+$ microvessel density in the tumor following CPA treatment

To evaluate the effect of metronomic CPA-dosing on the density of newly formed vessels in the tumor, the tumor was removed at either day 6, 7, 8, 9, 10, 11 or 12 after tumor-inoculation from the mice orally treated with *metronomic CPA dosing (Group A)*. The tumors were excised and snap-frozen in OCT compound (Sakura Fintechnical, Tokyo, Japan) by dry-iced acetone. Frozen samples were cut into sections of 10-μm thickness in a cryostat (Leica Microsystems, Solms, Germany), mounted on a glass slide and dried in air. The samples were sequentially fixed by incubation in cold acetone, 1:1 acetone/chloroform and cold acetone for 5 min (each treatment), washed with PBS (pH 7.4) and blocked with 5% BSA in PBS for 30 min at room temperature. After washing with PBS, samples were incubated overnight with FITC-labeled rat anti-mouse CD31 at 4 °C. After washing with PBS, the number of microvessels was determined by fluorescence microscopy (Axioimager A1, Zeiss, Oberkohen, Germany). The microvessel density was evaluated according to the method previously demonstrated with minor modification [34].

2.7. Intratumoral distribution of fluorescence-labeled liposomes

To evaluate the effect of CPA dosing on intra-tumoral distribution of intravenously injected SL, DiI-labeled SL (5 mg phospholipids/kg) were injected either on day 5 or day 11 after tumor inoculation, into the mice orally treated with different doses of CPA (20 or 60 mg/kg). Mice were sacrificed 24 h after the SL injection, and tumors were excised and snap-frozen in OCT compound by dry-iced acetone. Frozen samples were cut into sections of 10-μm thickness in a cryostat (Leica Microsystems, Solms, Germany), mounted on a glass slide and dried in air. Samples were directly observed by using a fluorescence microscopy (Axioimager A1) to evaluate the intratumoral distribution of liposomes. After the observation, the samples on the glass slide were stained with anti-mouse CD31 Ab as described above.

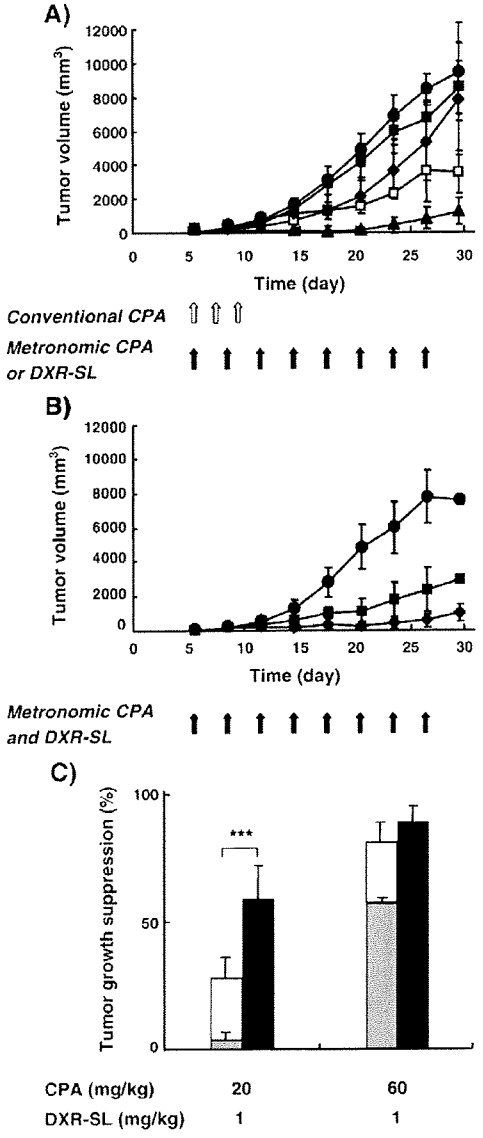

Fig. 1. Comparison of monotherapy and combination therapy with CPA and DXR-SL in early-stage solid tumor growth. (A) Monotherapy: Control (●), conventional CPA dosing (MTD) (▲), CPA (20 mg/kg) (■), CPA (60 mg/kg) (□), DXR-SL (1 mg/kg) (◆). (B) Combination therapy: Control (●), CPA (20 mg/kg) plus DXR-SL (1 mg/kg) (■), CPA (60 mg/kg) plus DXR-SL (1 mg/kg) (◆). (C) Index of tumor-growth suppression: The bars indicate the index of tumor-growth suppression by monotherapies at different doses of CPA (gray bar) and DXR-SL (white bar), and by combination therapy by CPA plus DXR-SL (filled bar). The data represent mean±S.D. ($n=5$). ***, $p<0.005$.

2.8. Toxicity assessment

To avoid the influence of tumorigenesis on toxicity assessment, normal C57BL/6 mice were used for toxicity assessment [15]. Mice received eight cycles of CPA or DXR-SL treatment with 3-day intervals. One cycle consisted of either oral administration of CPA (20 or 60 mg/kg) or intravenous injection of DXR-SL (1 mg/kg). After treatment was initiated, body weight was measured every third day.

Total number of white blood cell (WBC) was determined according to the method previously reported [5]. Blood was collected from a different set of mice via retro-orbital puncture on day 6, 10, 15 and 24 after treatment was begun. After washing with cold PBS twice by centrifugation for 5 min at 300 ×g and 4 °C, blood cells were blocked with 1% BSA in PBS for 15 min at room temperature and then incubated with primary Ab (rat monoclonal anti-mouse CD45 Ab) for 30 min. After washing with cold PBS, samples were incubated for an additional 30 min with secondary Ab (FITC-labeled rabbit anti-rat IgG heavy- and light-chain polyclonal Ab). WBC number was determined using flow cytometry (Guava EasyCyte Mini System, GE Healthcare, CA, USA).

2.9. Statistics

All values are expressed as the mean±S.D. Statistical analysis was performed with a two-tailed unpaired t test using GraphPad InStat software (GraphPad Software, CA, USA). The level of significant was set at $p<0.05$.

3. Results

3.1. Antitumor effect of combined therapy

We elucidated whether metronomic CPA-dosing can promote the efficacy of DXR-SL thus achieving a synergistic antitumor effect without severe adverse effects. When treatment began on day 5 after tumor inoculation, monotherapy with CPA (20 mg/kg) or DXR-SL (1 mg/kg) showed very little antitumor effect (Fig. 1A). At higher dose (60 mg/kg), monotherapy with CPA induced significant antitumor effect, but the effect was lower than that of conventional CPA dosing (MTD) (Fig. 1A). Combination of metronomic CPA-dosing (20 or 60 mg/kg) with DXR-SL (1 mg/kg) achieved a marked antitumor effect (Fig. 1B), the higher CPA dose producing a stronger antitumor effect in combination with DXR-SL. The index of tumor suppression is presented in Fig. 1C. The data indicate that the combination of the metronomic *lower dose* CPA-dosing (20 mg/kg) with DXR-SL (1 mg/kg) produced a synergistic antitumor effect, whereas the combination of metronomic *higher dose* CPA-dosing (60 mg/kg) with DXR-SL (1 mg/kg) produced an additive effect.

We extended our study of the combination chemotherapy to larger tumors (approximately 1000 mm^3), 12 days after inoculation. Monotherapy with DXR-SL showed almost no antitumor effect (Fig. 2A). Monotherapy with the *higher dose* CPA (60 mg/kg) showed a slight antitumor effect, while monotherapy with the *lower dose* CPA (20 mg/kg) showed almost no antitumor effect (Fig. 2A). Combination of *high dose* CPA (60 mg/kg) with DXR-SL (1 mg/kg) achieved a substantial antitumor effect (Fig. 2B). By contrast, combination of the *lower dose* CPA (20 mg/kg) with DXR-SL (1 mg/kg) did not show any antitumor effect. The index of tumor suppression is presented in Fig. 2C. The combination *higher dose* CPA (60 mg/kg) and DXR-SL (1 mg/kg), produced a synergistic effect against the larger tumor.

3.2. Density of $CD31^+$ microvessels in tumors treated with metronomic CPA dosing

The density of $CD31^+$ microvessels in the tumor was determined from fluorescence microscopy images of four to five tumors (Fig. 3).

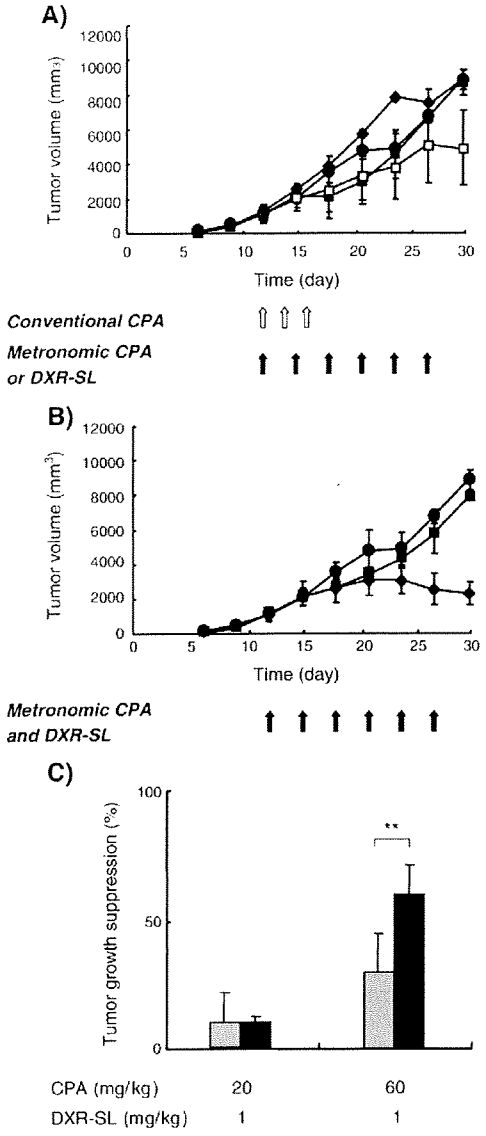

Fig. 2. Comparison of monotherapy and combination therapy with CPA and DXR-SL in late-stage solid tumor growth. (A) Monotherapy: Control (●), CPA (20 mg/kg) (■), CPA (60 mg/kg) (□), DXR-SL (1 mg/kg) (◆). (B) Combination therapy: Control (●), CPA (20 mg/kg) plus DXR-SL (1 mg/kg) (■), CPA (60 mg/kg) plus DXR-SL (1 mg/kg) (◆). (C) Index of tumor-growth suppression: The bars indicate the index of tumor-growth suppression by monotherapies at different doses of CPA (gray bar) and DXR-SL (white bar). The white bars do not show up because monotherapy with DXR-SL had no significant therapeutic effect. ● represents combination therapy by CPA plus DXR-SL. The data represent mean ± S.D. ($n=5$). **, $p<0.01$.

Sequential oral (metronomic) doses of CPA (20 mg/kg or 60 mg/kg) were given on day 5, 8 and 11 after tumor inoculation. One day after the start of the first treatment (on day 6 after tumor-inoculation), the density of CD31$^+$-microvessels was decreased only at the higher CPA dose (60 mg/kg). Interestingly, the densities tended to increase as of the second day after the first treatment (day 7) but this tendency vanished after the second treatment on day 8. The second treatment initially normalized the density of CD31$^+$-microvessels to control levels and then microvessel density started to increase again. The third treatment on day 11 did not normalize CD31$^+$-microvessel density on day 12.

The effect of metronomic CPA dosing on the density of CD31$^+$-microvessels was also checked in the larger tumors 12 days after inoculation (i.e., *metronomic CPA dosing, Group B*). No significant changes in tumor microvasculature were detected throughout day 13 to 19 after tumor inoculation (data not shown).

It is noteworthy that the density of CD31$^+$-microvessels in the control tumors (without treatment) tended to decrease in a time after tumor inoculation dependent manner (Fig. 3). This might be due to a difference in proliferation rate between tumor cells and endothelial cells, the aggressive tumor cells growing much faster than the endothelial cells.

3.3. Effect of CPA dosing on the distribution and accumulation of SL in the solid tumor

To gain more insight in the underlying mechanism of the synergistic antitumor effect observed in Figs. 1 and 2, we investigated the effect of CPA dosing on the accumulation and distribution of co-administered DiI-labeled SL in the tumor. Either on day 6 or 12 after tumor inoculation (one day before SL injection), the tumor sections were stained with FITC-labeled anti-CD31 Ab and examined for FITC (green) and DiI (red) fluorescence (Fig. 4A and B). The area density of DiI-labeled SL accumulated in the tumors was measured as the proportion of pixels having a fluorescence intensity value equal to or greater than the corresponding threshold on the basis of fluorescence microscopic digital images. The amount of SL in the tumor without treatment was set as control.

In the smaller tumors (on day 5; approximately 50 mm^3), the lower CPA dosing resulted in a markedly enhanced accumulation of SL in the tumor (Fig. 4A and C) and a far broader distribution of SL around the CD31$^+$ microvessels in the tumor (Fig. 4A). The higher CPA dose did not enhance the SL accumulation into the tumor as same as the lower dose did (Fig. 4A and C). In the larger tumors (on day 12; approximately 1000 mm^3), the CPA dosing resulted in enhanced accumulation of SL in the tumor (Fig. 4B and C) and a distribution of SL around the CD31$^+$ microvessels (Fig. 4B). The lower CPA dose enhanced the SL accumulation into the tumor relative to the higher dose (Fig. 4B and C). It appears that the lower CPA dose strongly affects the tumor vasculature and simultaneously induces extravasation of SL into the tumor tissue compared to the higher CPA dose (Fig. 4C). Also, the vasculature in the massively growing tumor appears to be much more sensitive to the CPA treatment than that in the matured tumor (Fig. 4A and B).

3.4. Toxicity of combination therapy

Because the presence of a tumor influences bone marrow function and because treatment of tumor-bearing mice with chemotherapeutic agents may unfavorably interfere with a correct interpretation of toxicity data, we determined the toxicity of the combination therapy of CPA and DXR-SL in non-tumor-bearing mice [15]. The toxicity of the

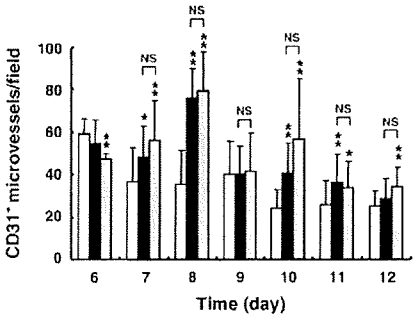

Fig. 3. CD31+-microvessel density in the tumor under a metronomic CPA-dosing schedule. Density of CD31$^+$ microvessels in the tumor was determined from fluorescence microscopic images taken from 4 to 5 tumors. CPA was orally administered on day 5, 8 and 11 after tumor-inoculation. Open column; control (without treatment). Filled column; CPA (20 mg/kg). Shaded column; CPA (60 mg/kg). *, $p<0.05$; **, $p<0.005$ versus Control. NS, not significant.